The Causes of Leaf Hydraulic Vulnerability and Its Influence on Gas Exchange in Arabidopsis thaliana

Christine Scoffoni, Caetano Albuquerque, Hervé Cochard, Thomas N. Buckley, Leila R. Fletcher, Marissa A. Caringella, Megan Bartlett, Craig R. Brodersen, Steven Jansen, Andrew J. Mcelrone, et al.

Plant Physiology Preview. Published on October 26, 2018, as DOI:10.1104/pp.18.00743

The causes of leaf hydraulic vulnerability and its influence on gas exchange in *Arabidopsis thaliana*

Christine Scoffoni[1,2], Caetano Albuquerque[3], Hervé Cochard[4], Thomas N. Buckley[5], Leila R. Fletcher[1], Marissa A. Caringella[1], Megan Bartlett[6], Craig R. Brodersen[7], Steven Jansen[8], Andrew J. McElrone[3,9], Lawren Sack[1]

[1] *Department of Ecology and Evolutionary Biology, University of California Los Angeles, 621 Charles E. Young Drive South, Los Angeles, California 90095, USA*
[2] *Department of Biological Sciences, California State University, Los Angeles, 5151 State University Drive, Los Angeles, California 90032, USA*
[3]*Department of Viticulture and Enology, University of California, Davis, CA 95616, USA*
[4]*Université Clermont-Auvergne, INRA, PIAF, F-63000 Clermont-Ferrand, France*
[5]*Department of Plant Sciences, University of California, Davis, CA 95616, USA*
[6]*Princeton Environmental Institute, Princeton University, NJ 08544, USA*
[7]*School of Forestry & Environmental Studies, Yale University, 195 Prospect Street, New Haven, CT 06511, USA*
[8]*Institute of Systematic Botany and Ecology, Ulm University*
[9]*USDA-Agricultural Research Service, Davis, CA 95616, USA*

One-sentence summary: Declines in leaf outside-xylem hydraulic conductance prior to turgor loss point contribute strongly to stomatal closure, and improve performance, survival and efficient water use during drought.

Author contributions: C. Scoffoni and L. Sack designed the study. C. Scoffoni, C. Albuquerque, H. Cochard, T.N. Buckley, L.R. Fletcher, M. Caringella, M.K. Bartlett, A.J. McElrone & L. Sack contributed to data collection and/or analyses. C. Scoffoni and L. Sack wrote the manuscript with input from all authors.

Corresponding Author:
Christine Scoffoni
California State University, Los Angeles
Department of Biological Sciences
5151 State University Drive, Los Angeles 90032, California
Email: cscoffo@calstatela.edu

Abstract

The influence of the dynamics of leaf hydraulic conductance (K_{leaf}) diurnally and during dehydration on stomatal conductance and photosynthesis remains unclear. Using the model species *Arabidopsis thaliana* (ecotype Col-0)., we applied a multi-tiered approach including physiological measurements, high-resolution X-ray micro-computed tomography, and modelling at a range of scales to characterize: (1) K_{leaf} decline during dehydration; (2) its basis in the hydraulic conductances of leaf xylem (K_x) and outside-xylem pathways (K_{ox}); (3) the dependence of its dynamics on irradiance; (4) its impact on diurnal patterns of stomatal conductance and photosynthetic rate; and (5) its influence on gas exchange and survival under simulated drought regimes. Arabidopsis leaves showed strong vulnerability to dehydration diurnally in both gas exchange and hydraulic conductance, despite lack of xylem embolism or conduit collapse above turgor loss point, indicating pronounced sensitivity of K_{ox} to dehydration. K_{leaf} increased under higher irradiance in well-hydrated leaves across the full range of water potential, but no shift in K_{leaf} vulnerability was observed. Modelling indicated that responses to dehydration and irradiance are likely attributable to changes in membrane permeability, and that a dynamic K_{ox} would contribute strongly to stomatal closure, improving performance, survival and efficient water use during drought. These findings for Col-0 provide a baseline for assessing variation across genotypes in hydraulic traits and their influence on gas exchange during dehydration.

Key words: aquaporins, drought, leaf water relations, plant modelling, pv-curves

Introduction

Plant growth requires a copious water supply because the rate of CO_2 uptake for photosynthesis depends on stomatal conductance, which results in transpiratory water loss. Because stomata close in dehydrating leaves, photosynthesis and growth depend on the efficiency of water replacement to the mesophyll. Thus, in the past two decades, many studies focusing on diverse species have shown the centrality of the plant hydraulic system in determining leaf-scale gas exchange and plant productivity (Sack and Holbrook, 2006; Brodribb et al., 2007; Scoffoni et al., 2016). Our aim was to test hypotheses for the dynamics of hydraulic traits and their influence on gas exchange during dehydration using the model species Arabidopsis. Establishing a framework for testing the influence of hydraulic traits in Arabidopsis can help address recent debates and open avenues for discovery of genetic associations in natural and mutant genotypes under moist conditions and during soil and/or atmospheric drought.

The leaf accounts for a large proportion of plant hydraulic resistance (Sack and Holbrook, 2006). Thus, theoretical and empirical studies have shown strong correlations of stomatal conductance (g_s) and photosynthetic rate (A_{max}) with leaf hydraulic conductance (K_{leaf}; determined as the flow rate divided by water potential driving force, in units mmol m^{-2} s^{-1} MPa^{-1}) across species under well-watered conditions (Nardini and Salleo, 2003; Brodribb and Holbrook, 2004; Sack and Holbrook, 2006; Scoffoni et al., 2016), and within given species during dehydration (Brodribb and Holbrook, 2006, 2007; Bartlett et al., 2016; Scoffoni and Sack, 2017). A high K_{leaf} enabling higher g_s and A_{max} could be achieved through a high vein length per area, larger and/or more numerous xylem conduits (and/or xylem pits), and more conductive mesophyll and bundle sheath anatomy and biochemistry (Brodribb et al., 2007; Choat et al., 2008; Caringella et al., 2015; Scoffoni et al., 2015; Scoffoni et al., 2016; Stewart et al., 2018). Yet, the linkages of K_{leaf} and gas exchange as leaves dehydrate to turgor loss point are still under debate. Early studies suggested that K_{leaf} decline drives stomatal closure under high vapor pressure deficits at mid-day (Brodribb and Holbrook, 2003a; Bucci et al., 2003) and during drought (Salleo et al., 2001; Brodribb and Holbrook, 2003b; Nardini and Salleo, 2003). Several recent studies suggested that in some species, K_{leaf} might not decline until embolism forms in the leaf vein xylem (Brodribb et al., 2016a; Brodribb et al., 2016b; Skelton et al., 2017), which for many species does not occur until past the point of stomatal closure and bulk leaf turgor loss (Brodribb et al., 2016b; Hochberg et al., 2017; Scoffoni et al., 2017a). Similarly, xylem wall collapse may drive K_{leaf} declines in pine needles and minor veins of an oak

species, but only below turgor loss point (Cochard et al., 2004a; Zhang et al., 2016). Avoiding K_{leaf} decline during transpiration when leaves are hydrated above turgor loss point has been suggested as adaptive, maintaining leaf water potential and open stomata, though at the risk of sustaining water potentials that would induce xylem cavitation under high vapor pressure deficits (Brodribb and Holbrook, 2006). Numerous studies in the last decade have shown that species differ in whether K_{leaf} declines at milder, similar or more severe leaf water potentials than at stomatal closure, and that K_{leaf} decline depends mechanistically on processes in multiple tissues—the venation, bundle sheath, and mesophyll pathways of liquid and vapor transport (reviewed by Scoffoni and Sack, 2017). Indeed, a meta-analysis of the literature found that on average, across species (and methods for K_{leaf} determination), K_{leaf} declined by 30-80% before turgor loss point (Scoffoni and Sack, 2017). Recent work focusing on partitioning leaf xylem and outside-xylem resistances during dehydration suggested the outside-xylem hydraulic conductance (K_{ox}) as the primary driver of K_{leaf} decline (Trifilo et al., 2016; Scoffoni et al., 2017a; Scoffoni and Sack, 2017), which could be triggered by the loss of cell connectivity, cell shrinkage, and/or changes in membrane aquaporin activity (Laur and Hacke, 2014b; Scoffoni et al., 2014; Scoffoni et al., 2017a), potentially mediated by effects of ABA in the bundle sheath (Pantin et al., 2013). A recent study in rice has attributed to K_{leaf} decline a strong causal role in driving stomatal closure during dehydration (Wang et al., 2018).

Debate has also focused on the light response of K_{leaf}. Previous studies have found many species to exhibit a rapid enhancement of K_{leaf} in response to increased irradiance (Sack et al., 2002; Nardini et al., 2005b; Tyree et al., 2005; Cochard et al., 2007; Scoffoni et al., 2008; Voicu et al., 2008; Guyot et al., 2012; Xiong et al., 2018), but not all (Sack et al., 2002; Gasco et al., 2004; Tyree et al., 2005; Scoffoni et al., 2008; Xiong et al., 2018). Activation of $PIP_{2,1}$ and $PIP_{2,2}$ aquaporins under high irradiance at high water potential has been shown to also enhance K_{leaf} in some (Cochard et al., 2007), though not all species (Voicu et al., 2009). A higher K_{leaf} under high light could potentially help buffer rapid changes in VPD and prevent stomata from closing (Cairns Murphy et al., 2012; Scoffoni et al., 2015). In Arabidopsis, one study estimated hydraulic conductance by pushing water into entire rosettes suspended underwater in a dark pressure chamber, and found it was higher for leaves acclimated to dark rather than high irradiance (Prado et al., 2013), though no study has investigated this response at the leaf level.

Here, we applied complementary physiological, imaging, and modelling approaches (Table 1) to assess K_{leaf} dynamics with dehydration and irradiance, and their role in driving diurnal patterns of gas exchange in Arabidopsis. We tested the hypotheses in Arabidopsis that K_{leaf}: (1) is high under well-hydrated conditions, but declines strongly during dehydration; (2) declines due to changes in K_{ox} but not xylem embolism formation or conduit collapse; (3) responds to irradiance; (4) influences diurnal patterns of stomatal conductance and photosynthetic rate; and (5) shows dynamics that confer higher water-use efficiency, and that would thus benefit plant performance under simulated soil drying.

Results

Leaf hydraulics and gas exchange and their responses to leaf dehydration and irradiance in Arabidopsis

Arabidopsis Col-0 exhibited high maximum leaf hydraulic conductance (K_{leaf}), stomatal conductance (g_s), minimum epidermal conductance (g_{min}), as well as light-saturated photosynthetic rate (A_{area}) (Figure 1, Figure 2, Table 2). The partitioning of hydraulic resistances in the leaf indicated a similar distribution of resistances in the xylem and outside-xylem pathways (45.6 vs. 54.4% respectively; Table 2).

Arabidopsis showed a strong vulnerability to dehydration in K_{leaf} and gas exchange (Figure 1). Notably, the range of water potential measured on intact plants diurnally, and on detached leaves during bench dehydration was similar (Figure 1, Figure 2). K_{leaf} responded non-linearly to dehydration, with steep declines before 50% loss of its initial K_{leaf} by -0.17 MPa (K_{leaf} P_{50}), and gradually slowing down its response to further dehydration (Table 2, Figure 1). Both g_s and A_{area} responded linearly to declining Ψ_{leaf} (Figure 2), reaching 50% loss of initial rates by -0.37 and -0.38 MPa respectively, and 95% loss at similar Ψ_{leaf} values of -0.71MPa (Table 2). At turgor loss point, K_{leaf} had declined by ca. 88%, and stomata were nearly fully closed (Table 2, Figure 1).

Leaves acclimated to high irradiance had significantly higher K_{leaf} values than leaves acclimated to low irradiance, with a 60% enhancement of K_{leaf} from low to high irradiance in well-hydrated leaves of Col-0. (Figure 1; *t*-test done on residuals of K_{leaf}, i.e., difference of observed values relative to those predicted from the best fit function through all data combined: ($K_{leaf} = 8.33 + 83.7 \times \exp(-(9.47 \times \Psi_{leaf}))$). Residuals for K_{leaf} were 7.4 mmol m^{-2} s^{-1} MPa^{-1} higher under high irradiance across the entire vulnerability curve ($p = 0.01$), 7.9 mmol m^{-2} s^{-1} MPa^{-1} higher

considering only leaves above turgor loss point (p = 0.01), and 13.9 mmol m^{-2} s^{-1} MPa^{-1} higher considering only leaves at hydration above -0.2MPa (p = 0.04). However, leaves acclimated to high and low irradiance were similar in their K_{leaf} P_{50} (-0.17 vs. -0.16 MPa respectively; Figure 1).

Diurnal responses of gas exchange

Photosynthetic and stomatal responses were measured over the course of two days, from 0900 to 1800. Our results showed that the diurnal pattern of whole-plant hydraulic conductance and gas exchange reflected the dynamics of Ψ_{leaf}, as evidenced by the strong trends of K_{plant}, g_s and A_{max} versus Ψ_{leaf} (r^2 = 0.45-0.81; p < 0.02; Figure 2). Of all the potential environmental drivers, vapor pressure deficit (VPD) most strongly correlated with g_s dynamics diurnally (r^2 = 0.18; p = 0.002; Supplemental Figure S1).

Independent effects analysis of potential drivers of diurnal dynamics in g_s, including environmental factors and Ψ_{leaf} showed that Ψ_{leaf} was the most important statistically, contributing 77% towards the diurnal variation (Supplemental Figure S2). The VPD contributed 11%, and temperature, PAR and time of day each contributed only 4% to the observed variation (Supplemental Figure S2).

Testing for vein xylem embolism and collapse during leaf dehydration using micro-computed tomography

We scanned leaves using *in vivo* micro-computed tomography for dehydrated plants to visualize potential xylem embolism. In 14/18 leaves attached to plants that spanned the observed range of Ψ_{leaf} (-0.05 to -0.87 MPa), no gas embolism was observed in major or minor veins (Figure 3). In 4/18 scans, we observed 1-2 embolized conduits in the midrib and/or secondary veins; notably, these leaves were not the most dehydrated (Ψ_{leaf} = -0.13 to -0.45 MPa; Figure 4; Table 3) but were within the same range as other leaves that did not exhibit embolism. In all three leaves that showed embolized midrib conduits, the embolism spanned the entire length of the scanned section, and we were unable to measure the total vessel length (Figure 4; Table 3). For two leaves, the embolized midrib conduit extended into a secondary vein. In the fourth leaf, an isolated embolised conduit in the secondary vein was observed (Figure 4, Table 3). All embolized conduits were of average diameter (Table 3; midrib conduit diameters measured under light microscopy ranged from 2.79 to 10.3 μm). No collapsed conduits were observed in midrib and secondary vein conduits at the

range of water potentials investigated. The resolution of the micro-CT scans was not sufficient to determine whether conduit collapse occured in higher-order veins.

Modelling the impact of embolism and collapse on K_x

Spatially explicit modelling of the leaf xylem (Table 1) showed that the very low level of observed xylem conduit embolism would reduce leaf xylem hydraulic conductance (K_x) by 1.2 to 4.7% (Table 3). Because resolution was not sufficient to determine whether conduit collapse occured in higher-order veins, we simulated the potential impact of such collapse if it had occurred. These simulations showed that if higher-order veins were to collapse to the same % of conduit diameter as recently reported for minor veins of *Quercus rubra* (Zhang et al., 2016), this would decrease K_x by 3-7.5% (Table 3). Under a more extreme scenario in which collapse of tertiary and minor veins caused a 50% decline in their conductivity, K_x would be reduced by 12-17% (Table 3), which would decrease K_{leaf} by 7- 9%.

Modelling the putative causes of K_{ox} *decline*

Spatially explicit modelling of the outside-xylem pathways using MOFLO 2.0 (Table 1) suggested that the main factor accounting for the decline in K_{ox} observed at -0.5 MPa was most likely reduction of cell membrane permeability in combination with an apoplastic barrier at the bundle sheath (Figure 5). Under high irradiance, an 80% reduction of cell membrane permeability would cause a 68.4% decrease in K_{ox}; adding an 80% reduction in cell connectivity would further decrease K_{ox} by 0.2 % (Figure 5). When performing these simulations with no apoplastic barrier at the bundle sheath, the impact of an 80% reduction of cell membrane permeability caused only a 24.5% decrease in K_{ox} (Figure 5). Simulating the impact of changes of temperature gradients due to light absorption changed the percent loss of K_{ox} by 1-3% across simulations (Supplemental Table S1). Finally, simulating the impact of cell shrinkage from full turgor to -0.5 MPa resulted in an increase in K_{ox} by 7 to 15%, due to the increase in vein density caused by leaf shrinkage and the consequent decrease in outside-xylem water flow pathlengths (Figure 5).

Partitioning the contribution of K_{leaf} *vulnerability to* g_s *decline*

In a transpiring leaf, a low Ψ_{leaf} would result from low water potentials proximally to the leaf (i.e., in the soil or roots; Table 1), and to the transpiration-driven water potential drop across the leaf,

which is greater, given K_{leaf} vulnerability. Thus, given that g_s declines with Ψ_{leaf}, K_{leaf} vulnerability will amplify the reduction of g_s at a given soil water potential and vapor pressure deficit. Using a partitioning analysis, we applied the observed parameters of g_s and K_{leaf} decline in Arabidopsis to compute the marginal % contribution of K_{leaf} vulnerability to the decline of g_s (Table 1). Our results showed that K_{leaf} vulnerability contributes strongly to g_s decline in transpiring leaves early in dehydration, due to amplification of Ψ_{leaf} decline; when g_s declines by 30%, 70% of this response is due to K_{leaf} vulnerability rather than low water potential proximal to the leaf (Figure 6). The contribution of K_{leaf} vulnerability to g_s decline remains >40% until g_s declined by 50%, and becomes less important as stomata approach full closure. When g_s has declined by 95%, the contribution of K_{leaf} vulnerability to g_s decline is < 1%.

Using the SurEau whole-plant physiology model to estimate the influence of K_{leaf} *decline on gas exchange, productivity and survival*

We tested the importance of K_{leaf} vulnerability prior to turgor loss point in reducing g_s and photosynthesis on plant carbon balance and survival in simulations using SurEau (Martin-StPaul et al., 2017) (Figure 7A-D; Table 1). In simulations, the experimentally observed K_{leaf} vulnerability caused an up to -0.36 MPa lower Ψ_{leaf} at midday under well-hydrated conditions (yellow and red lines), compared to constant K_{leaf} simulations (light and dark blue lines) (Figure 7B). This lower Ψ_{leaf} in turn reduced g_s and cumulative CO_2 assimilation ($A_{n,\,tot}$) by up to 62 and 17% respectively under well-hydrated conditions (Figure 7A-B), but cumulative water-use efficiency (calculated as $A_{n,\,tot}$/total transpiration) increased by 28% (inset in Figure 7B). Given finite soil water supply in these simulations, this higher water-use efficiency led to up to 24% higher $A_{n,\,tot}$ over the entire course of the simulated drought. Indeed, because K_{leaf} vulnerability results in lower g_s during the early stage of the drought, the soil water potential (approximated as nightime Ψ_{leaf} in Figure 7B) is maintained at higher levels as drought ensues, leading to the maintenance of higher g_s during later drought (Figure 7A). Additionally, because Ψ_{leaf} does not drop as fast during the course of the drought, these simulations showed that given K_{leaf} vulnerability, the onset of leaf xylem embolism occurs later during drought such that plants survive up to 6 days longer under drying soil (Figure 7D). These simulations resulted in similar findings whether or not K_{root} was set as vulnerable or constant, highlighting K_{leaf} vulnerability as a main driver of improved water-use efficiency, $A_{n,\,tot}$ and survival during soil drying.

Drought tolerance in Arabidopsis

Arabidopsis Col-0 exhibits low leaf mass per area, a high degree of area shrinkage during dehydration, high minimum epidermal conductance (g_{min}), high osmotic potential at full turgor and turgor loss point, low modulus of elasticity and relative water content at turgor loss point (Table 1).

Discussion

Our results demonstrate a potential strong role for outside-xylem pathways in the decline of K_{leaf} with leaf dehydration, contributing to stomatal closure and the reduction of photosynthetic rate in *Arabidopsis thaliana* (Col-0). Strong declines in K_{leaf} were associated with declines in K_{plant}, g_s and A_{area}, at water potentials where no significant embolism was observed using microCT. The absence of leaf xylem embolism before stomatal closure and hydraulic decline point to changes in outside-xylem pathways as the cause of observed K_{leaf} decline and imply no functional role of xylem dysfunction in this species' response of gas exchange to leaf dehydration. Modelling showed that K_{leaf} vulnerability has a strong causal role in determining stomatal closure, and further, that K_{leaf} vulnerability would improve plant carbon balance and survival during drought.

Drivers of leaf hydraulic conductance decline during dehydration

Our results suggest that changes in outside-xylem pathways are the main drivers of the response of K_{leaf} to dehydration in Arabidopsis. MicroCT imaging showed that embolism was rare in major vein xylem conduits and nonexistent in minor veins. Only one or two embolized conduits (representing on average 6-11% of the conduits in the midrib) were found in 4/18 samples, with no trend of embolism with increasing water stress prior to turgor loss point. This low vulnerability to embolism in leaves parallels findings for Arabidopsis inflorescence stems, which have P_{50} values lower than -2.5 MPa (Tixier et al., 2013). The few rare observed leaf vein xylem emboli likely arose from methodological artifacts. In the 3/4 samples in which embolized conduits were observed, the embolized conduit spanned the entire section. One possibility is that air may have entered the conduit when plants were removed from the soil for dehydration, if air entered conduits from damaged roots, and conduits were continuous into the major veins of scanned leaves. Similarly, air may have entered when the two leaves were excised from the plant for initial water

potential measurement, if conduits spanned from these leaves to others in the rosette including the scanned leaves. Alternatively, these few embolisms could be the result of defects in the development of these conduits (Pickard, 1981; Tyree et al., 1994). Indeed, we found a single isolated embolism event occured in a secondary vein of one of our samples. Such isolated embolism events have been reported in leaf veins of other angiosperm species (Scoffoni et al., 2017b) and stem xylem (Brodersen et al., 2013; Choat et al., 2015; Choat et al., 2016).

MicroCT imaging did not reveal any conduit collapse in the midrib or secondary veins across the range of observed water potentials. Since the resolution of the microCT imaging did not permit assessment of xylem conduit collapse in higher-order veins, we tested the potential effect of collapse of minor veins on K_{leaf} using a spatially explicit model of the leaf vein system. These simulations suggested that if xylem conduit collapse in the tertiary and minor veins were to occur within the range of water potentials in which K_{leaf} declined, this collapse would have a quantitatively small effect, i.e., causing <10% decline in K_{leaf} at -0.5MPa. This finding was consistent with previous model results showing that extreme collapse of minor veins would cause K_{leaf} to decline only by up to 4% for four diverse species (Scoffoni et al., 2017b). Previous studies found collapse of xylem conduits in pine needles and the minor veins of oak leaves, but only past turgor loss point, and suggested this could act as a circuit breaker to protect the stem xylem from embolism formation (Cochard et al., 2004a; Zhang et al., 2016). An early decline in outside-xylem pathways would act in a similar way, hastening stomatal closure, before xylem collapse would occur (Scoffoni et al., 2017a; and see following sections). Past turgor loss point, the Arabidopsis leaf undergoes drastic shrinkage in area and thickness, and it is likely that xylem in the midrib and higher-order veins would collapse, especially as the Arabidopsis xylem cell walls are helicoidal, and mostly consisting of thick primary walls (Figure 8). Future studies are needed to investigate the collapse of xylem and its influence on the rehydration capacity of strongly dehydrated leaves.

Response of leaf hydraulic conductance to dehydration and coordination with gas-exchange

In Arabidopsis, we did not observe any embolism in leaf xylem conduits prior to, or even moderately past the point of stomatal closure and turgor loss point. This finding is consistent with recent work on tomato and grapevine showing stomata closed before any embolism were observed using an optical visualization technique (Hochberg et al., 2017; Skelton et al., 2017). Here, we confirm this finding for the first time using microCT on Arabidopsis. This finding is also consistent

with a growing body of literature showing that typically no xylem embolism is observed prior to turgor loss point (Charra-Vaskou et al., 2012; Delzon and Cochard, 2014; Bouche et al., 2016; Brodribb et al., 2016b; Scoffoni et al., 2017a; Scoffoni et al., 2017b). A recent study on sunflower showed that xylem embolism occurs after turgor loss point even in plants that acclimate to drought: plants grown under water-limited conditions adjusted osmotically and had a more negative turgor loss point (-0.3 MPa shift), and leaf xylem P_{50} also shifted to a more negative value (-0.6 MPa shift) (Cardoso et al., 2018).

The diurnal variation observed in stomatal conductance (g_s) and net photosynthetic rate per leaf area (A_{area}) was strongly driven by leaf water status, i.e., Ψ_{leaf}, as shown by our model-fitting analyses. Further, our analyses indicated that the dynamics of Ψ_{leaf}, and thus of g_s and A_{area} were strongly driven by the dehydration-induced decline of K_{leaf}, in turn, resulting from changes in outside-xylem pathways. Thus, we found that in Arabidopsis, K_{leaf} declines more rapidly than g_s with dehydration, increasing the ratio of g_s/K_{leaf}, such that transpiration would amplify the decline in Ψ_{leaf}, and consequently that of g_s. Indeed, 40-65% of g_s decline was attributable to K_{leaf} decline, for leaves dehydrated to less than 50% of stomatal closure. For more strongly dehydrated leaves, given their reduced stomatal conductance, the transpiration-driven amplification of Ψ_{leaf} and g_s decline by K_{leaf} vulnerability are small, and declining Ψ_{leaf} due to low soil water potential and/or exogenous signals such as ABA or sugar production would be responsible for driving stomata to full closure. The direct mechanisms for stomatal closure with declining Ψ_{leaf} require further research. While most proximally, stomatal closure relates to solute transfer from guard cells to pavement cells, this could be driven by declining cell volume, turgor, osmotic concentration or water potential, in the epidermis and/or mesophyll, partially or fully mediated by ABA accumulation, which in turn may be associated with declining cell volume and K_{leaf} decline in dehydrating leaves (McAdam and Brodribb, 2016; Sussmilch et al., 2017; Sack et al., 2018). Indeed, ABA signaling may contribute to stomatal closure both directly at the guard cells and also by contributing to K_{leaf} decline in dehydrating leaves by reducing cell membrane permeability in the bundle sheath and mesophyll via changes in aquaporin expression (Shatil-Cohen et al., 2011; Pantin et al., 2013). Indeed, our MOFLO 2.0 simulations showed that K_{ox} decline was best explained by reduced cell membrane permeability and to a lesser extent, cell connectivity. In Arabidopsis, stress-induced changes in cell membrane permeability, mediated by aquaporins, can have a strong impact on root hydraulic conductance (Javot and Maurel, 2002).

Alternatively, some studies have suggested that photosynthetic rate and carbon sink activities could regulate stomata and plant hydraulics (Nikinmaa et al., 2013; Körner, 2015; Rockwell et al., 2018). Indeed, this is well known in cropping systems such as grapevine, where the presence of strong sinks such as fruits have been shown to stimulate photosynthesis (Hofäcker, 1978; Petrie et al., 2000). Recent studies have found that excess cellular sugar concentrations under high irradiance, and/or during dehydration could trigger stomata closure (Nikinmaa et al., 2013; Rockwell et al., 2018). Excess sucrose may be transported to the guard cells by the transpiration stream, and the subsequent increase in osmolytes at the guard cell apoplast could induce stomatal closure in some species, especially during periods of high photosynthetic rates (Lu et al., 1995; Lu et al., 1997; Kang et al., 2007a; Kang et al., 2007b). Indeed, the increase in sucrose concentration at the guard cells could act as more than a simple osmolyte, as it can depolarize the guard cell plasma membrane, activating potassium channels (Jarzyniak and Jasiński, 2014), and an increase in the level of sugar-sensing enzymes in the guard cells can accelerate stomatal closure by stimulating ABA production (Kelly et al., 2013; Van Houtte et al., 2013; Li et al., 2016; Li et al., 2018; Medeiros et al., 2018). Additionally, excess sucrose concentrations can decrease K_{ox} and thus K_{leaf}, potentially via deactivation of aquaporins (Kelly et al., 2017).

In conclusion, K_{leaf}, g_s and A_{area} show a coordinated decline during leaf dehydration in Arabidopsis, with a potentially strong direct effect of declining K_{leaf} in inducing stomatal closure via a decrease in water potential. The decline in K_{leaf} and stomatal conductance may be jointly driven by accumulation of sugar and/or ABA accumulation in dehydrating leaves, or K_{leaf} declines may contribute to this accumulation. Future studies are needed to decipher the exact sequence of events leading stomata to close.

Putative role of K_{ox} *decline in improving plant carbon balance, water-use efficiency and survival during drought*

Why would the water transport pathways outside the xylem decline in efficiency during dehydration prior to turgor loss point if this reduces gas exchange? Results from SurEau simulations indicated that a vulnerable K_{ox} (and thus K_{leaf}) above turgor loss point leads to greater water-use efficiency, and cumulative CO_2 assimilation, as well as protection of xylem from embolism, and increased plant survival during drought. Simulated plants with K_{ox} declining prior to turgor loss point operated on average at a lower K_{ox} value than plants with a K_{ox} held constant

(set to the average value measured at Ψ_{leaf} of-0.1 to -0.2 MPa, i.e., the range at which g_s was at its maximum). This dynamic K_{ox} with water potential caused an up to 60% decline in g_s but only an up to 12% decline in CO_2 assimilation, resulting in a higher water-use efficiency and greater overall assimilation when considered over the entire period of soil drying. This benefit for low K_{ox} raises the question of why plants should invest in a high K_{ox} (or K_{leaf}) in maximally hydrated leaves. Indeed, high K_{leaf} values at Ψ_{leaf} above -1.0MPa have at times been neglected when constructing vulnerability curves (Blackman et al., 2012; Blackman et al., 2014) under the presumption that leaves simply do not operate at such high water potentials in planta. However, a high K_{ox} (and thus K_{leaf}) in well-hydrated leaves which declines during dehydration prior to turgor loss point would offer advantages; it would enable high g_s and greater CO_2 assimilation under well-watered conditions. This would be particularly beneficial for a short-lived species such as Arabidopsis, which is required to grow rapidly when water availability is high. Previous studies have found that maximum K_{ox} (and K_{leaf}) was high and declined rapidly with water potential in herbs (Scoffoni et al., 2011; Nolf et al., 2016; Scoffoni et al., 2017a) than long-lived drought tolerant chaparral trees (Scoffoni et al., 2017a). Ephemeral species such as Arabidopsis, or desert plants with short-lived leaves, would especially benefit from high CO_2 assimilation rates, and thus high K_{leaf} after a rainfall event, and "gear down" by reducing K_{leaf} and thus transpiration rates when water becomes scarce, to improve their water-use efficiency and survive longer under soil drying (Grubb, 1998). In these simulations, root hydraulic vulnerability had a small effect on water-use efficiency in Arabidopsis. The much greater effect of leaf over root is due to the very high proportion of hydraulic resistance in the leaf (85.7%), due to the lack of stem in the vegetative phase of this rosette species. The hydraulic vulnerability of roots and their influence on the control of gas exchange is still under debate given experimental challenges. Debate is ongoing over whether root xylem is highly vulnerable (Hacke and Sauter, 1996; Hacke et al., 2000), or resistant (Rodriguez-Dominguez et al., 2018) to xylem embolism. However, just as in leaves (Scoffoni et al., 2017a), the root extra-xylem flow pathways might be more vulnerable. In grapevine, lacunae formation in fine root cortical cells may cause a strong decline in K_{root} under drying-soil conditions, which would help decouple the plant from drying soil and preserve its vascular system from embolism (Cuneo et al., 2016). Notably, plant competition for soil water is not simulated in the SurEau model. As such, we assume that plants have evolved to efficiently utilize soil water, and not overspend it (Cowan, 1982; Buckley et al., 2017b).

The light response of leaf hydraulic conductance in Arabidopsis

Maximum K_{leaf} for well-hydrated leaves often increases in response to light; this response has been found for 15 of 30 species tested, in species of 23 plant families (Sack et al., 2002; Gasco et al., 2004; Tyree et al., 2005; Cochard et al., 2007; Scoffoni et al., 2008; Voicu et al., 2008; Guyot et al., 2012; Xiong et al., 2018). Further, in some species, the light enhancement of K_{leaf} is reduced in dehydrated leaves, or, equivalently for those species, K_{leaf} declines with dehydration more steeply under high irradiance (Guyot et al., 2012). In Arabidopsis, a previous study suggested that the hydraulic conductance of entire rosettes of Arabidopsis had increased when acclimated to low rather than high irradiance (Prado et al., 2013). In our experiments using the evaporative flux method, we found significantly higher K_{leaf} values throughout the range of water potentials tested for leaves acclimated to high irradiance, with a 60% enhancement of K_{leaf} from low to high irradiance in well-hydrated leaves of Col-0. Discrepancies between these results may have arisen due to methodological differences, given that in the study of Prado et al. (2013), hydraulic conductance was measured by pushing water inward through the stomata of entire rosettes suspended under water in darkness within a pressure chamber.

Notably, the light enhancement in K_{leaf} found in Arabidopsis did not result in a shift in P_{50}. This finding indicates a proportional shift to lower values under low irradiance, throughout the range of water potentials, contrary to findings for four woody species in which leaves acclimated to high irradiance were more vulnerable to K_{leaf} decline with dehydration (Guyot et al. 2012). The light enhancement of K_{leaf} would provide a greater hydraulic supply to meet the demand of leaves acclimated to high irradiance, i.e., given strong and rapid dynamics of air temperature and humidity and wind, and thus higher vapor pressure deficit and leaf boundary layer conductance. Further, given strong transient dehydration during transpiration under these conditions, the higher K_{leaf} would contribute to rapid mesophyll rehydration at high water potential and thus enable the recovery of g_s and photosynthetic rate. The light enhancement of K_{leaf} could be caused by stronger temperature gradients throughout the leaf under high light and/or changes in aquaporin expression (Cochard et al., 2007). Our simulations of K_{ox} under low and high light using MOFLO 2.0 indicated that K_{leaf} would be minimally enhanced by temperature gradients in the leaf caused by light absorption, pointing to a role for aquaporins instead. This is consistent with the molecular evidence that aquaporin expression is sensitive to light (Cochard et al., 2007; Ben Baaziz et al., 2012) and

that mutltiple aquaporin isoforms are involved in a range of responses such as K_{leaf} decline during drought and K_{leaf} light enhancement (Cochard et al., 2007; Pou et al., 2013; Laur and Hacke, 2014b, a). Furthermore, aquaporins may also be involved in cell rehydration (Marco et al., 2016). Finally, aquaporins have also been suggested to play a role in a rapid enhancement of K_{leaf} when Arabidopsis is suddenly exposed to low relative humidity, compensating for the increased evapotranspiration, and allowing stomata to remain open (Levin et al., 2007).

Contribution of hydraulic traits to Arabidopsis thaliana whole-plant physiology

Arabidopsis Col-0 has high values of K_{leaf}, g_s and A_{area} relative to previously published values of diverse angiosperm species (Flexas et al., 2013; Scoffoni and Sack, 2017), and displays strong sensitivity in K_{leaf} and gas exchange to dehydration. This physiological behavior is consistent with Arabidopsis' ruderal ecology, establishing and producing flowers and seeds in open or disturbed habitats in spring/early summer (Koornneef et al., 2004). The high values of K_{leaf} were driven by an especially high K_{ox} (106 mmol m^{-2} s^{-1} MPa^{-1}). This high K_{ox} is not untypical in herbs; in *Salvia canariensis*, maximum K_{ox} reached 231 mmol m^{-2} s^{-1} MPa^{-1} (Scoffoni et al., 2017a). Notably, a high K_x,K_{ox} and K_{leaf} are often achieved with allocation to substantial vein length per area (VLA), which increases flow paths in parallel within the xylem and reduces flow distance outside the xylem (Sack and Scoffoni, 2013); Arabidopsis possesses a relatively low VLA but flow distance is strongly reduced by its very thin leaf, which would also reduce K_{ox} (Brodribb et al., 2007; Buckley et al., 2015). Furthemore, a high aquaporin activity, and/or cell wall permeability especially at the bundle sheath could potentially influence K_{ox}; across several Arabidopsis mutants, maximum K_{leaf} was associated with an anatomical index of bundle sheath conductivity (Caringella et al., 2015). The high K_x value could potentially arise from xylem structure, i.e., the numbers and sizes of xylem cells within minor veins (Caringella et al., 2015; Stewart et al., 2018), in combination with high conductance between xylem conduits. Indeed, our TEM imaging showed very little secondary lignification of xylem conduits throughout the midrib and other vein orders (Figure 8), such that the bulk of midrib conduit walls are effectively one large pit membrane (i.e., primary unlignified wall) with water potentially leaking throughout the surface, a structure that would strongly reduce pit wall resistance and thus total xylem resistance (Choat et al., 2008).

Arabidopsis Col-0 also exhibits strong drought sensitivity, with its very low leaf mass per area (Wright et al., 2004), a very high degree of area shrinkage during dehydration (58% shrinkage

when dry), high minimum epidermal conductance (g_{min}), very high osmotic potential at full turgor, low modulus of elasticity and relative water content at turgor loss point, and a turgor loss point that is among the highest values reported across angiosperm species (Bartlett et al., 2012), similar to that of the water potential at stomatal closure (g_{s95}) and at 88% loss of K_{leaf}, around -0.7MPa. This detailed characterization of Arabidopsis Col-0 hydraulics traits, and their dynamics during leaf dehydration and implications for whole-plant responses highlights useful avenues for high throughput phenotyping, and the elucidation of genetic mechanisms controlling these key traits, which would be loci for manipulation of gas exchange and drought tolerance.

Material and methods

Plant material and growth conditions

Measurements were performed on *Arabidopsis thaliana* Col-0 (ecotype Colombia), hereafter refered to as Arabidopsis, grown continuously from December 2015 through November 2016. We grew *Arabidopsis thaliana* in a climate-controlled greenhouse at the University of California, Los Angeles. Seeds were sown in lawns in pots (3.13" width x 4.88"length x 2.31" deep) in soil (1:1:2:1:1 mixture of washed plaster sand, loam, peat moss, perlite, vermiculite), and cold-acclimated at 4°C for three days in a chamber, then brought to the temperature-controlled greenhouse (minimum, mean, and maximum values for temperature, 19.3°C, 22.5°C, and 33.2°C; for humidity, 24%, 63%, and 92%; for irradiance (from 0900 to 1600), 11.2, 169, 1369 µmol photons m^{-2} s^{-1}). We recognize that many researchers often grow Arabidopsis in growth chambers under <300 µmol photons m^{-2} s^{-1} irradiance, and future work should consider the variation in leaf physiology, morphology and anatomy driven by this lower irradiance. We chose to grow Arabidopsis in a greenhouse setting where plants are exposed to light fluctuations, with temporary high light peaks, as is experienced in the field. Indeed, this has been shown to impact plant growth (Poorter et al., 2016). Further, growing plants under such high irradiance means that these were not light-limited, and thus, our findings can be compared with those for other species grown without light limitation, as is typical in studies of plant hydraulic physiology.

When plants had true leaves after approximately one week, they were thinned to one individual per pot. Plants were watered regularly to keep soil moist. After approx. 6 weeks, at which points plants had >10-20 leaves, mature and healthy leaves were chosen for gas exchange, hydraulic and x-ray micro-computed tomography measurements.

Leaf hydraulic conductance

Pots were transported to the laboratory, watered and enclosed overnight in plastic bags filled with wet paper towels to ensure a saturated atmosphere. To obtain a vulnerability curve spanning a range of leaf water potential (Ψ_{leaf}), well-hydrated and dehydrated leaves were measured. To obtain K_{leaf} values at high Ψ_{leaf}, mature and healthy leaves were directly cut at their base under water and their petioles placed in a petri dish containing ultra-pure water (0.22 μm Thornton 200 CR; Millipore) prior to being connected to the evaporative flux system described below. To obtain K_{leaf} values at low Ψ_{leaf}, individuals were removed from the soil and dehydrated on the bench for 0.25-2 hours, after which they were placed in bags which had previously been exhaled into, within a second bag filled with wet paper towels, to ensure high vapor and CO_2 concentration, to reduce stomatal opening and facilitate equilibration for 30 min. Two leaves were then measured for initial Ψ_{leaf}, using a pressure chamber (Plant Moisture Stress Model 1000; PMS Instrument Co, Albany, OR, USA), with a grass fitting in the compression lid; for a few leaves with round petioles, silicon adaptors were used (Shatil-Cohen et al., 2011). On average, the two leaves measured for initial Ψ_{leaf} differed by 0.051 MPa ± 0.008 standard error. A third mature and healthy leaf from the dehydrated individual was measured for K_{leaf}. After the leaf petiole was cut under water, it was gently wrapped with parafilm and connected via tubing to a water source on a balance (±10 μg, models XS205 and AB265; Mettler Toledo, Columbus, OH, USA), which logged the flow rate into the leaf every 5 s to a computer. The leaf was placed over a fan and under a light source (>1000 μmol $m^{-2}s^{-1}$; model 73828, 1000 W UV filter; SearsRoebuck, Hoffman Estates, IL, USA). A water bath was placed between the leaf and the light to avoid overheating the leaf, which was kept between 23 and 28°C as measured using a thermocouple (Cole-Parmer). After a minimum of 30 min to ensure light acclimation (Scoffoni et al., 2008) and once the flow had stabilized with no upward or downward trend, the average steady state flow rate for the last 5 min was recorded and leaf temperature was measured (Cole-Parmer). The leaf was rapidly removed from the system, its petiole dabbed dry, and placed in a bag which had previously been exhaled into. The bagged leaf was placed into a second bag filled with wet paper towels, and left to equilibrate for 30 min, after which final Ψ_{leaf}, was measured. Leaf area was manually traced onto paper, scanned, and measured using ImageJ software (version 1.46r; National Institutes of Health). Leaf hydraulic conductance (K_{leaf}) was calculated as the flow rate divided by the leaf water potential driving force (the water

potential of the water fed to the petiole [0 MPa] minus measured Ψ_{leaf}), normalized by leaf area and corrected for the dependence of water viscosity on temperature (to a reference value of 25°C; Weast, 1974 ; Yang and Tyree, 1993); this correction also approximately applies for the temperature dependence of vapor phase transport across this range of temperature (Buckley, 2015). Leaf hydraulic vulnerability curves were obtained as the plot of K_{leaf} vs. the most negative Ψ_{leaf} experienced by the leaf (either the initial or final).

K_{leaf} vulnerability curves were measured under very low laboratory irradiance (light source off; <3 μmol photons m^{-2} s^{-1}) and high irradiance (>1000 μmol $m^{-2}s^{-1}$). Measurements in very low and high irradiance were performed on the same day using leaves taken from the same individuals when possible, i.e.,when two leaves from the same individual were mature and healthy. Notably, the aim of this experiment was to test for a rapid light enhancement of K_{leaf} for high-light–grown individuals. Future studies are needed to investigate the plasticity in K_{leaf} and other physiological and morphological traits for Arabidopsis across different light growth regimes, as found to be important in a study of species of Hawaian lobeliads (Scoffoni et al., 2015).

Leaf xylem hydraulic conductance

Leaf xylem hydraulic conductance was measured for six leaves (taken from six different individuals) using the vacuum pump method (Kolb et al., 1996; Nardini et al., 2001; Sack et al., 2004; Scoffoni and Sack, 2015; Trifilo et al., 2016). Briefly, individuals were rehydrated in the laboratory overnight, and kept in dark plastic bags filled with wet paper towels to ensure high humidity. The next morning, a leaf was cut off the plant under ultra-pure water and placed in a petri dish over a white light transilluminator table (Model TW, UVP, Upland, CA, USA) to allow visualization of the fourth-order veins (=minor veins). Using a fresh scalpel, 8-15 cuts per cm^2 of leaf area were made to the lamina, severing minor veins, to ensure that outside-xylem pathways would be bypassed (Sack et al., 2004; Nardini and Salleo, 2005; Nardini et al., 2005b; Sack et al., 2005). Great care was taken to avoid cutting major veins; if they were cut by accident, the leaf was discarded. Once the cuts were made, the leaf petiole was wrapped with parafilm and inserted through a small rubber stopper that had been perforated using a cork borer. The small rubber stopper was then connected to a tube fitting connected to silicone tubing (ColeParmer, Vernon Hills, IL, USA). The rubber stopper allowed a good seal around the petiole without crushing. We obtained a vacuum tight seal by tightening the tubing around the rubber stopper with zipties and

sealing the petiole to the exposed end of the rubber stopper using super glue (Loctite 409 glue; Henkel Corp., Los Angeles, CA, USA) with accelerator (Loctite 712 accelerator). Leaves were placed inside a vacuum flask with a thermocouple (Cole-Parmer) connected by a fourway valve to a vacuum pump (Gast) and a high-precision pressure gauge (±0.002 MPa; J4605 Marsh/Bellofram; Marshall Instruments Inc., Anaheim, CA, USA).

We applied five increasing levels of partial vacuum, resulting in absolute pressures between 0.06 and 0.02 MPa, and recorded the flow rate of water entering the leaf from a water source on a balance (±10 µg, models XS205 and AB265; Mettler Toledo, Columbus, OH, USA). The average flow rate of the last 5 min of stability for a given pressure was recorded, along with the temperature. The flow rate was normalized to 25°C correct for the temperature response of the viscosity of water (Weast, 1974 ; Yang and Tyree, 1993). Leaf xylem hydraulic conductance (K_x) was calculated as the slope of the flow rate vs. pressure, and normalised by leaf area, measured at the end of the experiment with a flatbed scanner. The percent hydraulic resistance in the leaf xylem (%R_x) and outside-xylem (%R_{ox}) were calculated as:

(1) $$\%R_x = \frac{1/K_x}{1/K_{leaf}} \times 100$$

(2) $$\%R_{ox} = 100 - \%R_x$$

Diurnal measurements of stomatal conductance, photosynthetic rate and whole plant hydraulic conductance as a function of leaf water potential

Diurnal measurements of light-saturated photosynthetic rate (A_{max}) and stomatal conductance (g_s) were performed in the greenhouse on 40 individuals on 10-11 November 2016 from 0900 to 1800 using a portable gas exchange system (LI-6400; LI-Cor, Lincoln, NE, USA). The chamber CO_2 was set at 400 ppm and irradiance at 1000 µmol m^{-2} s^{-1} photosynthetically active radiation, and leaf to air vapor pressure deficit was maintained between 0.4 and 0.6 kPa. Measurements were taken after the leaf had equilibrated in the chamber for 10 min; A_{max} and g_s were logged 5 times at 10-sec intervals, and these five measurements were averaged. We checked that 10 min was sufficient equilibration time; n = 7 leaves were kept in the chamber for an additional five minutes; no significant differences were found between values taken at 10 vs. those taken at 15 min (paired t-test; p = 0.08). To verify g_s measurements, additional measurements were taken using a

porometer on the abaxial side of the leaf (Delta-T Devices; Cambridge, UK) on 10-11 November 2016 from 0900 to 1800. As expected, the g_s values obtained from the LICOR and porometer were within the same range of values and thus were pooled together during the analyses.

At the end of the measurement, the leaf was excised with a razor blade and immediately placed in a sealable bag (Whirl-Pak, Nasco, Fort Atkinson, WI, USA), which had been previously exhaled in, and the bagged leaves were placed in a second bag filled with wet paper towels. After at least 30-min equilibration, Ψ_{leaf} was measured using a pressure chamber as described above.

Whole-plant hydraulic conductance (K_{plant}; mmol m^{-2} s^{-1} MPa^{-1}) was estimated under the assumption that soil water potential was fully saturated throughout the day (thus, Ψ_{soil} = 0 MPa). Though we did not directly measure Ψ_{soil}, plants were well-watered and soil was always moist. Thus, K_{plant} was determined from the stomatal conductance obtained from the porometer data described above (measurements performed under ambient light irradiance), ambient VPD at the time of measurement, and leaf water potential:

$$K_{\text{plant}} = \frac{g_s \times VPD}{\Psi_{\text{soil}} - \Psi_{\text{leaf}}} \quad (3)$$

X-ray micro-computed tomography

To visualize leaf vein xylem embolism and tissue shrinkage, we used X-ray micro-computed tomography (microCT) at the synchrotron at the Advanced Light Source (ALS) in Berkeley, California (Beamline 8.3.2). We imaged the xylem within the midrib and lamina tissues in 18 leaves of a range of leaf water potential from 9 individuals in February 2016 at 1.27-μm resolution. Three additional individuals were further scanned in November 2016 at a higher resolution of 0.638 μm to check for potential collapse in xylem conduits of the midrib. Arabidopsis individuals grown as described above were transported as carry-on in a plane to ALS. Individuals were fully rehydrated at the start of the experiment, and whole plants were removed from the soil and dehydrated on the bench for different times to obtain a range of water potentials, and equilibrated in double-sealed plastic bags for 30 min, after which two leaves were excised to obtain initial leaf water potential. Two of the leaves remaining attached to the plant were juxtaposed within a styrofoam holder and 0.653-0.869 mm length scans were made of their midrib and surrounding lamina at the center of each leaf. A small piece of copper wire was attached at the center of the

leaves to help center the samples for scanning. Kapton tape (DuPont, Wilmington, DE, USA) was used to tape the leaves and the copper wire to the styrofoam holder to minimize sample movement during the scan. The styrofoam with the sample enclosed was placed in a Plexiglass cylinder, attached to a custom-built aluminium sample holder mounted on an air-bearing stage, and wet paper towels were placed above the sample in the Plexiglass cylinder to minimize evaporation during the measurement. At the end of the measurement, final leaf water potential was recorded and leaf areas were measured. No significant differences in water potential before and after the measurement were observed (paired *t*-test; $p = 0.70$; $n = 8$). Scans were made at 20-23 keV in the synchrotron X-ray beam, and rotated 180° with the instrument to enable visualization of the full 3D internal structure of the leaf. Scans took 5-10 min to complete depending on the scan area selected. Three-dimensional volume renderings were made using the AVIZO 8.1.1 software (VSG Inc., Burlington, MA, USA), and used to count the number of embolized conduits in the entire sample and different vein orders. For the four samples that showed embolism, we measured the length of the embolized conduit and the widths of both conduit axes at three locations along the sample length. We also visualized for each section the water-filled conduits within the midrib and secondary veins to observe any potential deformation or collapse.

Using ImageJ software (version 1.46r; National Institutes of Health), we measured lamina tissue and cell dimensions on three cross-sectional images randomly selected in the middle of each sample. For each image, we measured thickness of the lamina and of each tissue, i.e., the abaxial and adaxial epidermises including the cuticle, and the palisade and spongy mesophyll, at three locations within the sample. We also measured the area, perimeter and diameters as well as the % intercellular airspace of palisade and spongy mesophyll cells.

Drought tolerance traits

The leaf turgor loss point, osmotic potential at full turgor, relative water content at turgor loss point and modulus of elasticity were calculated from a pressure-volume curve constructed using 29 leaves from 20 individuals previously rehydrated overnight (Supplemental Figure S3). Initial leaf mass was obtained for each single leaf before dehydration to a range of Ψ_{leaf}. Leaf water potentials were measured with a pressure chamber after 30 min of equilibration in bags with high humidity, after which the leaf mass was measured again, along with leaf area, before it was placed in a drying

oven at 70°C and measured for dry mass after 72 hours. Pressure-volume curve parameters were obtained following standard protocols (Sack and PrometheusWiki, 2010).

We measured the minimum epidermal conductance (=cuticular plus residual stomatal conductance; g_{min}) on nine mature leaves from nine individuals in June 2016 by following a standard protocol (Sack et al., 2010). Individual leavess were rehydrated covered in plastic in the laboratory the night before measurements. The next day, nine leaves excised, their cut petioles were sealed with wax, and their fresh mass and leaf area were measured, before dehydration for an hour taped to a fishing line above a fan, to ensure stomatal closure. Leaves were then repeatedly taken off the fan and bagged and measured for mass every 20 min. After eight measurements were obtained for a given leaf, its area was measured again. The g_{min} was calculated as the slope of mass over time divided by the average mole fraction vapor pressure deficit (VPD) during the measurement and normalized by the average of the initial and final leaf area given shrinkage with dehydration during measurement. VPD was calculated from the temperature and relative humidity measurements obtained from a weather station (HOBO Micro Station with Smart Sensors, Onset, Bourne, MA, USA). Finally, each individual leaf was dried in an oven at 70°C for three days, and dry mass and area were obtained to calculate leaf dry mass per hydrated area (*LMA*; in g m^{-2}) and the percent area shrinkage in the dried leaf relative to the hydrated leaf (PLA_{dry}; %).

Leaf anatomy

Data for leaf venation and leaf cross-sectional anatomy of Col-0 to aid with interpretation of microCT images were obtained from a previous study (Caringella et al., 2015).

To visualize xylem conduit walls, transmitted electron microscopy (TEM) was performed on three leaves from three Col-0 individuals in Germany. Small samples (ca. 2 mm wide and 8 mm long) from leaf midribs (and surrounding mesphyll) were cut under water and fixed in glutaraldehyde (2.5% glutaraldehyde, 0.1 mol phosphate, 1% saccharose, ph 7.3) overnight. After being washed in phosphate buffer and post-fixed with 2% OsO4, samples were dehydrated in a series of propanol solutions (30%, 50%, 70%, 90% and three times 100%). Samples were finally immersed in 1.2-propylenoxide (CAS-Nr. 75.56-9, Fontenay-sous-Bois, France) and gradually embedded in Epon resin (Sigma-Aldrich, Steihneim, Germany) and polymerized at 60°C for 48 h. Ultra-thin sections (<90 nm thick) were made with a Leica Ultracut UTC microtome (Leica Microsystems GmbH, Wetzlar, Germany) and placed on copper slot grids). Observations were

made using a JEOL 1400 TEM (JEOL, Tokyo, Japan) at an accelerating voltage of 120 kV. Images were taken with a digital camera (Soft Imagign System, Münster, Germany).

Modelling of hydraulic function across scales from tissues to whole plant

We applied a framework of four models across scales to compute the mechanisms underlying K_{leaf} decline inside and outside the xylem, the causal role of K_{leaf} decline in driving stomatal closure, and the implications for gas exchange under simulated drought regimes (Table 1).

We first estimated the causal importance of mechanistic drivers of K_{leaf} decline using spatially explicit models of the leaf veins (K_LEAF; Cochard et al., 2004b; Scoffoni et al., 2017b) and outside-xylem pathways (MOFLO 2.0; Buckley et al., 2017a). Using K_LEAF, we tested whether xylem embolism and/or conduit collapse could explain the observed decline in K_{leaf}. We first tested for the impact of the embolisms observed with microCT imaging in the midrib and secondary veins on the xylem hydraulic conductance (K_x) and ultimately K_{leaf} (see Supplemental Methods for more information on model parameterization; Supplemental Table S2). We tested the potential effect of the collapse of tertiary and minor vein conduits on K_x under two scenarios: (1) a "realistic" impact of conduit collapse on conduit conductivity (13% decline in tertiary and minor vein conductivity, similar to that observed in *Quercus rubra* at turgor loss point by Zhang et al., 2016), and (2) a more severe conduit collapse scenario which would induce 50% decline in tertiary and minor vein conduit conductivity (see Supplemental Methods). Using MOFLO 2.0, we investigated the potential drivers of decline in outside-xylem hydraulic conductance with dehydration. We simulated the impact of an 80% decline in cell membrane permeability, and/or decline in cell-to-cell liquid phase hydraulic connectivity given the anatomical changes due to cell shrinkage at -0.5 MPa under different scenarios: (1) with or without an apoplastic barrier to liquid-phase water transport across the bundle sheath, (2) under either no light or with an irradiance of 600 μmol m^{-2} s^{-1} photosynthetically active radiation to clarify a potential role of transdermal temperature gradients (Supplemental Methods; Supplemental Table S2).

We then quantified the direct influence of K_{leaf} decline on g_s decline with dehydration, using a partitioning approach. We first considered the empirical maximum likelihood functions relating K_{leaf} and g_s to leaf water potential:

(4) $$g_s = -451 \times |\Psi_{leaf}| + 339$$

(5) $$K_{leaf} = 6.83 + 81.4\exp(-7.56 \times |\Psi_{leaf}|)$$

Ψ_{leaf} is in turn a function of g_s, K_{leaf}, soil water potential (Ψ_{soil}) and the water vapor mole fraction gradient (Δw):

(6) $$\Psi_{leaf} = \Psi_{soil} - \Delta w \frac{g_s}{K_{leaf}}$$

As Ψ_{leaf} declines during leaf dehydration, the resulting declines in g_s and K_{leaf} lead to changes in their ratio, g_s/K_{leaf}. If K_{leaf} declines more rapidly than g_s with Ψ_{leaf}, such that the ratio g_s/K_{leaf} increases, the decline in Ψ_{leaf} will be amplified, and consequently so will the decline in g_s itself. Therefore, K_{leaf} decline with dehydration would contribute to stomatal closure. The fraction of g_s decline with Ψ_{leaf} that can be attributed to K_{leaf} decline, F, is

(7) $$F = \frac{\frac{\partial g_s}{\partial K_{leaf}} \frac{\partial K_{leaf}}{\partial \Psi_{leaf}}}{\frac{\partial g_s}{\partial \Psi_{leaf}}} \quad ,$$

where the partial derivative in the numerator is the sensitivity of g_s to Ψ_{leaf} with Ψ_{soil} and Δw held constant (1.5 kPa). That partial derivative is given by

(8) $$\frac{\partial g_s}{\partial K_{leaf}} = \frac{\partial g_s}{\partial \Psi_{leaf}} \frac{\partial \Psi_{leaf}}{\partial K_{leaf}} = \frac{\partial g_s}{\partial \Psi_{leaf}} \left[-\Delta w \left(\frac{1}{K_{leaf}} \frac{\partial g_s}{\partial K_{leaf}} - \frac{g_s}{{K_{leaf}}^2}\right)\right]$$

Solving for $\partial g_s/\partial K_{leaf}$ gives

(9) $$\frac{\partial g_s}{\partial K_{leaf}} = \frac{\frac{\partial g_s}{\partial \Psi_{leaf}} \frac{g_s \Delta w}{{K_{leaf}}^2}}{1 + \frac{\partial g_s}{\partial \Psi_{leaf}} \frac{\Delta w}{K_{leaf}}} = \frac{\frac{\partial g_s}{\partial \Psi_{leaf}} \frac{g_s}{K_{leaf}}}{\frac{\partial g_s}{\partial \Psi_{leaf}} + \frac{K_{leaf}}{\Delta w}}$$

Combining 7 and 9 gives F as

(10) $$F = \frac{\frac{\partial K_{leaf}}{\partial \Psi_{leaf}} \frac{g_s}{K_{leaf}}}{\frac{\partial g_s}{\partial \Psi_{leaf}} + \frac{K_{leaf}}{\Delta w}}$$

Finally, using a simplified discrete-time soil–plant hydraulic model (SurEau; Martin-StPaul et al., 2017), we estimated the influence of K_{leaf} decline on stomatal closure under varying

simulations of soil and atmospheric drought. We simulated transpiration, stomatal conductance, cumulative photosynthetic rate, cumulative water-use efficiency, water potential and the percent loss of xylem hydraulic conductance (PLC) daily and during the course of soil drying until plant death (i.e., PLC = 100%). We performed these simulations following four different scenarios: (1) K_{leaf} and K_{root} were both vulnerable to dehydration prior to turgor loss point (using the function of K_{leaf} vs. Ψ_{leaf} measured with the EFM, and the vulnerability of K_{root} obtained from that of K_{leaf} and K_{plant}, assuming no stem resistance in Arabidopsis; Supplemental Figure S4); (2) K_{leaf} was vulnerable but not K_{root} (K_{root} was kept constant until xylem embolism occurred in the root); (3) K_{root} was vulnerable but not K_{leaf} (K_{leaf} was kept constant until xylem embolism occurred in the leaf); and (4) neither K_{leaf} nor K_{root} were vulnerable to dehydration (i.e., both K_{leaf} and K_{root} were kept at constant values until xylem embolism occurred) (Supplemental Methods; Supplemental Table S3).

Statistics

We selected functions for the responses of K_{plant}, K_{leaf}, g_s and A_{max} to Ψ_{leaf} using a maximum likelihood framework (Burnham and Anderson, 2002; Sack et al., 2006). For the g_s and A_{max} curve fitting, extremely low values at the beginning or end of the day when stomata were shut in well-hydrated leaves (Ψ_{leaf} > -0.01 MPa) were discarded, and likely represented the effects of the mechanical advantage of epidermal cells preventing stomatal opening in turgid leaves (Guyot et al., 2012); these points represented 3/63 and 2/26 of the points for g_s and A_{max} respectively. We selected the maximum likelihood model using the optim function in R 3.4.1 (http://www.r-project.org;). We fitted four types of functions to the curves, as previously used in the literature (Scoffoni et al., 2012), where Y= K_{leaf}, A_{area} or g_s, and Ψ_{leaf} is leaf water potential: linear ($Y = a\ \Psi_{leaf} + y_0$), two-parameter sigmoidal ($Y = a / (1+ e^{(-(\Psi leaf - x0)/b)})$), logistic ($Y = a / (1+ (\Psi_{leaf} / x_0)^b)$), and exponential ($Y = y_0 + a \times e^{-(b \times \Psi leaf)}$). We estimated the maximum Y value by extrapolating to Ψ_{leaf} = 0 and, as indices of decline with dehydration, the Ψ_{leaf} at which maximum Y values decreased by 50% and 95%. Because the best-fit function for the K_{leaf} vulnerability curve was exponential and the Y value at Ψ_{leaf} = 0 was extrapolated to a very high unrealistic value, we also estimated the maximum K_{leaf} by averaging all points above -0.1 MPa (K_{max}), as has been typically done in the literature (i.e., Sack et al., 2003; Nardini et al., 2005a; Brodribb and Jordan, 2008; Scoffoni et al., 2008; Scoffoni et al., 2015).

To test for an effect of light on K_{leaf}, we selected the best-fit function for the response of K_{leaf} to Ψleaf, combining data for laboratory irradiance and high irradiance treatments, using a maximum-likelihood framework as explained above. We then calculated the residual variation for each leaf, subtracting the measured K_{leaf} (and irradiance) from the predicted K_{leaf} at the given Ψ_{leaf}, based on the best fit. We then performed a *t*-test on the residuals obtained for the high vs. low irradiance leaves across the entire range of Ψ_{leaf}, as well as just for points above turgor loss point, and for well-hydrated leaves (above -0.2MPa).

To determine the contribution of each correlated predictor variables (Time, PAR, Temperature, VPD, Ψ_{leaf}) to the observed variation in g_s diurnally, we applied independent effects analysis (Murray and Conner, 2009) using the hier.part function in R.3.4.1.

Acknowledgements

We thank Weimin Dang, Dula Parkinson, and Jessica Smith for technical assistance, and the University of California, Los Angeles, Plant Growth Facility and the Advanced Light Source in Berkeley, California (Beamline 8.3.2). This work was supported by the U.S. National Science Foundation (award nos. 1457279 and 1557906), a Humboldt Research Postdoctoral Fellowship, a CAPES/Brazil Fellowship, and the International Wheat Yield Partnership. The Advanced Light Source is supported by the Director, Office of Science, Office of Basic Energy Sciences, of the US Department of Energy under Contract no. DE-AC02-05CH11231.

Figure captions

Figure 1. Decline of leaf hydraulic conductance (K_{leaf}) measured under high (>1000 μmol photons m^{-2} s^{-1}) or low (< 3 μmol photons m^{-2} s^{-1}) irradiance. The maximum likelihood function is shown for K_{leaf} vulnerability acclimated under high light ($K_{\mathrm{leaf}} = 6.83 + 81.4\exp(-7.56 \times |\Psi_{\mathrm{leaf}}|)$), and low light ($K_{\mathrm{leaf}} = 8.98 + 84.2\exp(-13.2 \times |\Psi_{\mathrm{leaf}}|)$). The dashed line respresents the water potential at 50% loss of K_{leaf} (similar in both treatments).

Figure 2. Plant hydraulic and gas exchange response to dehydration in Arabidopsis. Decline of the whole plant hydraulic conductance (K_{plant}; A), stomatal conductance (g_s; B) and light-saturated photosynthetic rate (A_{area}; C) with dehydration. Each point represents a different measured leaf. K_{plant} was obtained from the porometer data by dividing transpiration by leaf

water potential (assuming soil water potential was at full saturation). The black fitted line in each pannel is the maximum likelihood function (exponential for $K_{\text{plant}} = 2.0 + 91.1 \exp(-7.75 \times |\Psi_{\text{leaf}}|)$; linear for $g_s = 339 - 451 \times |\Psi_{\text{leaf}}|$, and $A_{\text{area}} = 14.4 - 19.2 \times |\Psi_{\text{leaf}}|$). The dotted grey line is the leaf water potential (Ψ_{leaf}) at 50% loss of maximum K_{plant}, g_s or A_{area}. Because trait values above -0.1 MPa were especially low (white circles), likely representing stomatal closure at those high water potentials (see *Methods*), we did not include these points in the line fitting.

Figure 3. Lack of embolism observed in midrib conduits of *Arabidopsis thaliana* (Col-0) across levels of dehydration as revealed by in vivo images of leaf midribs subjected to progressive dehydration using micro-computed tomography (A-C). Water-filled cells appear in light grey in microCT. If air-filled (i.e., embolized) conduits were present, they would appear as black in the xylem portion of the midrib. There was no embolism, as shown in these images by the red arrows pointing at the entirely light grey midrib xylem. The leaf water potential (Ψ_{leaf}) has been provided for each image. The inset in (A) represents a leaf midrib cross-section imaged under light microscopy, with the red arrow pointing to the xylem tissue (dark blue conduits).

Figure 4. Rare embolisms were observed in a few individual leaves. In two samples, an embolized conduit was observed in the midrib; it continued into a secondary vein (A, F; the embolized conduits are depicted in yellow). The embolized conduit in the midrib and secondary vein can be seen in cross-sections (B, D, G, I) and longitudinal sections of the microCT scan (C, E, H, J). The arrows point to the embolized conduit (appearing as black in the microCT image). Because of the two dimensionalities of these sections, embolism in the midrib and secondary vein might appear disconnected (C, E). Note that while the embolism was present in only one conduit per cross-sectional image, multiple conduits spanned the length of the midrib and secondary vein (as can be observed in K, where two conduits can be seen connected to one another). Most likely, a first conduit in the midrib embolized, and all the conduits directly connected to that one upstream embolized after. In one sample, an embolized conduit was observed isolated in the secondary vein (L-N), while in another sample, an embolized conduit was observed spanning the midrib length (O-Q).

Figure 5. Results from simulations using a spatially explicit model of leaf outside-xylem water to test for potential drivers of the decline in K_{ox} in dehydrating leaves transport (MOFLO 2.0, see Table 1 and *Methods*). The K_{ox} was first computed based on the decline of observed cell size and air space alone (grey bars), which resulted in an increase in K_{ox} (negative percent loss of K_{ox}; mainly due to shortening of pathways from the veins to stomata). We then modelled K_{ox} decline according to three scenarios (though always including the effect of tissue dimensional changes): an 80% decline at -0.5MPa in (1) cell connectivity (red bars), (2) cell membrane permeability (blue bars), and (3) cell wall thickness (black bars). All simulations were run with (Ap; darker color) or without an apoplastic barrier (No Ap; lighter color) at the bundle sheath cells. The yellow star on the *x*-axis represents the % observed K_{leaf} decline at -0.5MPa (measured with the evaporative flux method, see *Methods*).

Figure 6. Model simulations mapping the contribution of the decline of leaf hydraulic conductance (K_{leaf}) decline to that of stomatal conductance (g_s) with dehydration (Table 1).

Figure 7. Daily simulated patterns of stomatal conductance (A), leaf water potential (B), cumulative CO_2 assimilation (C) and the percent loss of leaf xylem hydraulic conductance (D) during the progression of a simulated soil drought (SurEau Model, see Table 1 and *Methods*). Four scenarios were modelled: (1) both leaf hydraulic conductance (K_{leaf}) and root hydraulic conductance (K_{root}) were vulnerable to dehydration prior to turgor loss point (yellow lines), (2) K_{leaf} was vulnerable, but not K_{root} (red lines), 3) K_{root} was vulnerable, but not K_{leaf} (light blue lines), or (4) neither K_{leaf} nor K_{root} was vulnerable (dark blue lines). The inset in (C) shows cumulative water-use efficiency (WUE; calculated as cumulative CO_2 assimilation (A) over total transpiration rate (E)) over time. Scenarios including a vulnerable K_{leaf} showed leaves that showed highest water-use efficiency, cumulative CO_2 assimilation and survived longer under drought conditions.

Figure 8. Transmitted-electron microscopy of *Arabidopsis thaliana* (Col-0) midrib cross-sections. In A, the entire xylem portion of the midrib can be seen. Black arrows point to the lack of secondary lignified wall around xylem conduits. These long primary wall sections can be observed in more detail in B. The white arrow points to a lignified portion of the secondary

xylem wall. We hypothesize that the xylem resistance through these deeply helicoidal xylem conduits is greatly reduced, as unlignified primary cells effectively work as one large pit membrane.

Supplemental Table and Figure captions

Supplemental Table S1. K_LEAF simulation inputs

Supplemental Table S2. Model inputs and simulation results from MOFLO 2.0.

Supplemental Table S3. SurEau inputs

Supplemental Figure S1. External environmental drivers of stomatal conductance measured diurnally in a greenhouse with a porometer.

Supplemental Figure S2. Leaf water potential is the main driver of observed diurnal variation in stomatal conductance.

Supplemental Figure S3. Pressure-volume curve for *Arabidopsis thaliana* (Col-0).

Supplemental Figure S4. Vulnerability curve of the plant (K_{plant}; brown), leaf (K_{leaf}; green) and root (K_{root}; yellow) hydraulic conductance.

Table 1. Modelling framework across scales to determine the underlying mechanisms linking K_{leaf} decline to gas exchange. Symbols: A_{area}= leaf photosynthetic rate; g_{min}= minimum epidermal conductance; g_{max}= maximum stomatal conductance; g_s= stomatal conductance; K_{leaf}= leaf hydraulic conductance; K_x= leaf xylem hydraulic conductance; K_{ox}= leaf outside-xylem hydraulic conductance; PLC= percent loss of hydraulic conductance; VPD= vapor pressure deficit; Ψ_{leaf}= leaf water potential.

Model	Purpose	Input	Output	Results
K_LEAF (Cochard et al., 2004; Scoffoni et al., 2017)	Model the influence of xylem embolism and potential conduit collapse on K_x and K_{leaf}	Leaf size, number of secondary veins and theoretical conductivities from the different veins orders at (1) at full turgor, and after accounting (2) for the decline caused by observed embolism in midrib and/or secondary veins, and (3) for the decline potentially caused by collapsed xylem conduits of tertiary and higher order veins (under a "realistic" collapsed scenario as observed in an oak species (Zhang et al., 2016) which caused 13% PLC, and a more severe scenario—causing 50% PLC)	Leaf xylem hydraulic conductance	Neither embolism nor xylem conduit collapse caused a decline in K_x substantial enough to explain the observed decline in K_{leaf}.
MOFLO 2.0 (Buckley et al., 2017)	Model the influence of changes in outside-xylem pathways on K_{ox} and K_{leaf}	Cell shrinkage and % intercellular airspace at -0.5MPa obtained from microCT, stomatal conductance (abaxial and adaxial), vapor pressure deficit and bulk leaf temperature. Simulations were performed under no light or 600 μmol m^{-2} s^{-1} photosynthetically active radiation, with or without an apoplastic barrier at the bundle sheath, and with or without an 80% decline in cell membrane permeability and/or cell connectivity.	Leaf outside-xylem hydraulic conductance	Reduction of cell membrane permeability in the context of an apoplastic barrier would account for most of the K_{leaf} decline observed at -0.5MPa. Temperature gradients through the leaf due to irradiance had little impact on K_{ox}.
Marginal contribution of *K* decline (refined from Rodriguez-Dominguez et al., 2016)	Quantify the influence of K_{leaf} decline on g_s decline	Parameters from the maximum likelihood function of g_s and K_{leaf} vs. Ψ_{leaf}, VPD set at a constant value (1.5 kPa), and a computed range of % g_s decline (0 to 100% decline in gs with Ψ_{leaf}).	Contribution of K_{leaf} decline to g_s decline with dehydration.	K_{leaf} decline explains most of the changes in g_s during mild to moderate dehydration.
SurEau (Martin-StPaul et al., 2017)	Quantify the influence of K_{leaf} decline on gas exchange in whole plant context during drought	Parameters from the maximum likelihood function of K_{leaf} vs. Ψ_{leaf}, parameters from the function of K_{root}vs. water potential, g_{min}, g_{max}, Farqhar's model inputs, PAR, air temperature, air humidity, time of day, transpiration under well-hydrated conditions, soil volume.	Soil water reserve, water potentials, transpiration rate, g_s, A_{area}, PLC.	Decline in K_{leaf} causes leaf water potential to drop, which in turn causes both g_s and A_{area} to decline under increasing VPD and decreasing soil water potential.

Table 2. Mean ± standard error for the physiological and anatomical traits measured for *Arabidopsis thaliana (col-0)*. Symbols: K_{max}: maximum leaf hydraulic conductance; K_x: leaf xylem hydraulic conductance; $\%R_{ox}$: percent resistance outside the leaf xylem; g_s: stomatal conductance; A_{max}: maximum light saturated photosynthetic rate; P_{50}, P_{88}, and P_{95}: leaf water potential at 50, 88 ns 95% decline in a given trait.

Trait	Units	Col-0
Hydraulics and gas exchange		
K_{max}	mmol m^{-2} s^{-1} MPa^{-1}	59.9 ± 1.76
$K_{leaf0.1\text{-}0.2MPa}$	mmol m^{-2} s^{-1} MPa^{-1}	33.1 ± 4.55
K_x	mmol m^{-2} s^{-1} MPa^{-1}	138.4 ± 14.5
K_{ox}	mmol m^{-2} s^{-1} MPa^{-1}	106
$\%R_{ox}$	%	54.4
$\%R_{leaf}$	%	85.7
g_s	mmol m^{-2} s^{-1}	339 ± 24.9
A_{max}	µmol m^{-2} s^{-1}	14.4 ± 2.72
K_{leaf} P_{50}	MPa	-0.17
g_s P_{50}	MPa	-0.38
A_{area} P_{50}	MPa	-0.37
K_{leaf} P_{88}	MPa	-0.72
g_s P_{95}	MPa	-0.71
A_{area} P_{95}	MPa	-0.71
Drought-tolerance traits		
Turgor loss point (TLP)	MPa	-0.73
Osmotic potential at full turgor ($\boldsymbol{\pi_o}$)	MPa	-0.63
Modulus of elasticity ($\boldsymbol{\varepsilon}$)	MPa	5.70
Relative water content at turgor loss point (RWC_{TLP})	%	84.1
Leaf mass per unit leaf area (LMA)	g m^{-2}	13.6 ± 0.89
Percent loss of area in a dry leaf (PLA_{dry})	%	57.9 ± 3.05
Minimum epidermal conductance (g_{min})	mmol m^{-2} s^{-1}	18.6 ± 1.33
Leaf anatomical traits		
Distance from vein to lower epidermis (VED)	mm	0.067 ± 0.002
Total vein length per area (VLA)	mm mm^{-2}	3.04 ± 0.08
Minor vein length per area (minor VLA)	mm mm^{-2}	1.79 ± 0.08
Major vein length per area (major VLA)	mm mm^{-2}	1.25 ± 0.05
$K_{t,\ midrib\ per\ leaf\ area}$	mmol m^{-1} s^{-1} MPa^{-1}	0.27 ± 0.12
$K_{t,\ minor\ per\ leaf\ area}$	mmol m^{-1} s^{-1} MPa^{-1}	0.003 ± 0.0008

Table 3. Observations of embolized conduits and dimensions from microCT and their simulated impact on leaf xylem hydraulic conductance using the spatially explicit K_LEAF model. Because we did not have the resolution to determine whether conduit collapse occurs in tertiary and minor veins, two simulations were performed based on minor vein conduit collapse observed in *Quercus rubra* (see *Methods*). Note that two leaves were imaged at each water potential (22 leaves total); embolism at the four water potentials below were only found in one of the two leaves tested at that water potential.

Leaf water potential (MPa)	Number of embolized conduits			Length of embolized conduit (µm)	Diameter of embolized conduit conduit (µm)		Simulated percent loss of xylem hydraulic conducance (%)		
	midrib	*2°*	*3°+*	*midrib*	*midrib*	*2°*	*Embolism only*	*Embolism + "realistic" 3°+ vein collapse (13% PLC)*	*Embolism + "severe" 3°+ vein collapse (50%PLC)*
-0.06	0	0	0	-	-	-	0	-	-
-0.08	0	0	0	-	-	-	0	-	-
-0.13	1	1	0	>898	7.3	8.7	7.13	9.99	19.1
-0.16	0	0	0	-	-	-	0	-	-
-0.18	2	2	0	258; >600	6.2; 5.3	5.2; 3.5	3.96	6.70	16
-0.45	0	1	0	-	-	5.2	0.96	3.12	9.1
-0.48	1	0	0	>850	5.9	-	1.16	3.96	13
-0.50	0	0	0	-	-	-	0	-	-
-0.69	0	0	0	-	-	-	0	-	-
-0.79	0	0	0	-	-	-	0	-	-
-0.87	0	0	0	-	-	-	0	2.82	12

Literature Cited

Bartlett MK, Klein T, Jansen S, Choat B, L. S (2016) The correlations and sequence of plant stomatal, hydraulic, and wilting responses to drought. Proceedings of the National Academy of Sciences of the United States of America **113:** 13098-13103

Bartlett MK, Scoffoni C, Sack L (2012) The determinants of leaf turgor loss point and prediction of drought tolerance of species and biomes: a global meta-analysis. Ecology Letters **15:** 393-405

Ben Baaziz K, Lopez D, Rabot A, Combes D, Gousset A, Bouzid S, Cochard H, Sakr S, Venisse JS (2012) Light-mediated K-leaf induction and contribution of both the PIP1s and PIP2s aquaporins in five tree species: walnut (Juglans regia) case study. Tree Physiology **32:** 423-434

Blackman CJ, Brodribb TJ, Jordan GJ (2012) Leaf hydraulic vulnerability influences species' bioclimatic limits in a diverse group of woody angiosperms. Oecologia **168:** 1-10

Blackman CJ, Gleason SM, Chang Y, Cook AM, Laws C, Westoby M (2014) Leaf hydraulic vulnerability to drought is linked to site water availability across a broad range of species and climates. Annals of Botany **114:** 435-440

Bouche PS, Delzon S, Choat B, Badel E, Brodribb T, Burlett R, Cochard H, Charra-Vaskou K, Lavigne B, Shan L, Mayr S, Morris H, Torres-Ruiz JM, Zufferey V, Jansen S (2016) Are needles of *Pinus pinaster* more vulnerable to xylem embolism than branches? New insights from X-ray computed tomography. Plant, Cell & Environment **39:** 860-870

Brodersen CR, McElrone AJ, Choat B, Lee EF, Shackel KA, Matthews MA (2013) In Vivo Visualizations of Drought-Induced Embolism Spread in *Vitis vinifera*. Plant Physiology **161:** 1820-1829

Brodribb TJ, Bienaime D, Marmottant P (2016a) Revealing catastrophic failure of leaf networks under stress. Proceedings of the National Academy of Sciences of the United States of America **113:** 4865-4869

Brodribb TJ, Feild TS, Jordan GJ (2007) Leaf maximum photosynthetic rate and venation are linked by hydraulics. Plant Physiology **144:** 1890-1898

Brodribb TJ, Holbrook NM (2003a) Changes in leaf hydraulic conductance during leaf shedding in seasonally dry tropical forest. New Phytologist **158:** 295-303

Brodribb TJ, Holbrook NM (2003b) Stomatal closure during leaf dehydration, correlation with other leaf physiological traits. Plant Physiology **132:** 2166-2173

Brodribb TJ, Holbrook NM (2004) Stomatal protection against hydraulic failure: a comparison of coexisting ferns and angiosperms. New Phytologist **162:** 663-670

Brodribb TJ, Holbrook NM (2006) Declining hydraulic efficiency as transpiring leaves desiccate: two types of response. Plant Cell and Environment **29:** 2205-2215

Brodribb TJ, Holbrook NM (2007) Forced depression of leaf hydraulic conductance in situ: effects on the leaf gas exchange of forest trees. Functional Ecology **21:** 705-712

Brodribb TJ, Jordan GJ (2008) Internal coordination between hydraulics and stomatal control in leaves. Plant Cell and Environment **31:** 1557-1564

Brodribb TJ, Skelton RP, McAdam SAM, Bienaime D, Lucani CJ, Marmottant P (2016b) Visual quantification of embolism reveals leaf vulnerability to hydraulic failure. New Phytologist **209:** 1403-1409

Bucci SJ, Scholz FG, Goldstein G, Meinzer FC, Sternberg LDL (2003) Dynamic changes in hydraulic conductivity in petioles of two savanna tree species: factors and mechanisms contributing to the refilling of embolized vessels. Plant Cell and Environment **26:** 1633-1645

Buckley TN (2015) The contributions of apoplastic, symplastic and gas phase pathways for water transport outside the bundle sheath in leaves. Plant Cell and Environment **38:** 7-22

Buckley TN, John GP, Scoffoni C, Sack L (2015) How Does Leaf Anatomy Influence Water Transport outside the Xylem? Plant Physiology **168:** 1616-1635

Buckley TN, John GP, Scoffoni C, Sack L (2017a) The sites of evaporation within leaves. Plant Physiology **173:** 1763-1782

Buckley TN, Sack L, Farquhar GD (2017b) Optimal plant water economy. Plant, Cell & Environment **40:** 881-896

Burnham KP, Anderson DR (2002) Model selection and multimodel inference, 2nd ed. Springer, New York, New York, USA.

Cairns Murphy MR, Jordan GJ, Brodribb TJ (2012) Differential leaf expansion can enable hydraulic acclimation to sun and shade. Plant, cell & environment **35**

Cardoso AA, Brodribb TJ, Lucani CJ, DaMatta FM, McAdam SAM (2018) Coordinated plasticity maintains hydraulic safety in sunflower leaves. Plant, Cell & Environment **0**

Caringella MA, Bongers FJ, Sack L (2015) Leaf hydraulic conductance varies with vein anatomy across *Arabidopsis thaliana* wild-type and leaf vein mutants. Plant Cell and Environment **38:** 2735-2746

Charra-Vaskou K, Badel E, Burlett R, Cochard H, Delzon S, Mayr S (2012) Hydraulic efficiency and safety of vascular and non-vascular components in Pinus pinaster leaves. Tree Physiology **32:** 1161-1170

Choat B, Badel E, Burlett R, Delzon S, Cochard H, Jansen S (2016) Non-invasive measurement of vulnerability to drought induced embolism by X-ray Microtomography. Plant Physiology **170:** 273-282

Choat B, Brodersen CR, McElrone AJ (2015) Synchrotron X-ray microtomography of xylem embolism in Sequoia sempervirens saplings during cycles of drought and recovery. New Phytologist **205:** 1095-1105

Choat B, Cobb AR, Jansen S (2008) Structure and function of bordered pits: new discoveries and impacts on whole-plant hydraulic function. New Phytologist **177:** 608-625

Cochard H, Froux F, Mayr FFS, Coutand C (2004a) Xylem wall collapse in water-stressed pine needles. Plant Physiology **134:** 401-408

Cochard H, Nardini A, Coll L (2004b) Hydraulic architecture of leaf blades: where is the main resistance? Plant Cell and Environment **27:** 1257-1267

Cochard H, Venisse JS, Barigah TS, Brunel N, Herbette S, Guilliot A, Tyree MT, Sakr S (2007) Putative role of aquaporins in variable hydraulic conductance of leaves in response to light. Plant Physiology **143:** 122-133

Cowan IR (1982) Water use and optimization of carbon assimilation. *In* Encyclopedia of plant physiology. 12B. Physiological plant ecology (eds Lange O. L., Nobel C.B., Osmond C.B. & Ziegler H.), Springer-Verlag, Berlin, pp 589–630

Cuneo IF, Knipfer T, Brodersen C, McElrone AJ (2016) Mechanical failure of fine root cortical cells initiates plant hydraulic decline during drought. Plant Physiology **doi:10.1104/pp.16.00923**

Delzon S, Cochard H (2014) Recent advances in tree hydraulics highlight the ecological significance of the hydraulic safety margin. New Phytologist **203:** 355-358

Flexas J, Scoffoni C, Gago J, Sack L (2013) Leaf mesophyll conductance and leaf hydraulic conductance: an introduction to their measurement and coordination. Journal of Experimental Botany **64:** 3965-3981

Gasco A, Nardini A, Salleo S (2004) Resistance to water flow through leaves of *Coffea arabica* is dominated by extra-vascular tissues. Functional Plant Biology **31:** 1161-1168

Grubb PJ (1998) A reassessment of the strategies of plants which cope with shortages of resources. Perspectives in Plant Ecology Evolution and Systematics **1:** 3-31

Guyot G, Scoffoni C, Sack L (2012) Combined impacts of irradiance and dehydration on leaf hydraulic conductance: insights into vulnerability and stomatal control. Plant, Cell & Environment **35:** 857-871

Hacke U, Sauter JJ (1996) Drought-induced xylem dysfunction in petioles, branches, and roots of Populus balsamifera L and Alnus glutinosa (L) Gaertn. Plant Physiology **111:** 413-417

Hacke UG, Sperry JS, Pittermann J (2000) Drought experience and cavitation resistance in six shrubs from the Great Basin, Utah. Basic and Applied Ecology **1:** 31-41

Hochberg U, Windt CW, Ponomarenko A, Zhang Y-J, Gersony J, Rockwell FE, Holbrook NM (2017) Stomatal closure, basal leaf embolism, and shedding protect the hydraulic integrity of grape stems. Plant Physiology **174:** 764-775

Hofäcker W (1978) Investigations on the photosynthesis of vines influence of defoliation, topping, girdling and removal of grapes Vitis **17:** 10-22

Jarzyniak KM, Jasiński M (2014) Membrane transporters and drought resistance – a complex issue. Frontiers in Plant Science **5:** 687

Javot H, Maurel C (2002) The role of aquaporins in root water uptake. Annals of Botany **90:** 301-313

Kang Y, Outlaw JWH, Fiore GB, Riddle KA (2007a) Guard cell apoplastic photosynthate accumulation corresponds to a phloem-loading mechanism. Journal of Experimental Botany **58:** 4061-4070

Kang Y, Outlaw WH, Andersen PC, Fiore GB (2007b) Guard-cell apoplastic sucrose concentration – a link between leaf photosynthesis and stomatal aperture size in the apoplastic phloem loader *Vicia faba* L. Plant, Cell & Environment **30:** 551-558

Kelly G, Moshelion M, David-Schwartz R, Halperin O, Wallach R, Attia Z, Belausov E, Granot D (2013) Hexokinase mediates stomatal closure. The Plant Journal **75:** 977-988

Kelly G, Sade N, Doron-Faigenboim A, Lerner S, Shatil-Cohen A, Yeselson Y, Egbaria A, Kottapalli J, Schaffer AA, Moshelion M, Granot D (2017) Sugar and hexokinase suppress expression of PIP aquaporins and reduce leaf hydraulics that preserves leaf water potential. The Plant Journal **91:** 325-339

Kolb KJ, Sperry JS, Lamont BB (1996) A method for measuring xylem hydraulic conductance and embolism in entire root and shoot systems. Journal of Experimental Botany **47:** 1805-1810

Koornneef M, Alonso-Blanco C, Vreugdenhil D (2004) Naturally occurring genetic variation in *Arabidopsis thaliana*. Annual Review of Plant Biology **55:** 141-172

Körner C (2015) Paradigm shift in plant growth control. Current Opinion in Plant Biology **25:** 107-114

Laur J, Hacke UG (2014a) Exploring *Picea glauca* aquaporins in the context of needle water uptake and xylem refilling. New Phytologist **203:** 388-400

Laur J, Hacke UG (2014b) The role of water channel proteins in facilitating recovery of leaf hydraulic conductance from water stress in *Populus trichocarpa*. Plos One **9**

Levin M, Lemcoff JH, Cohen S, Kapulnik Y (2007) Low air humidity increases leaf-specific hydraulic conductance of Arabidopsis thaliana (L.) Heynh (Brassicaceae). Journal of Experimental Botany **58:** 3711-3718

Li Y, Xu S, Gao J, Pan S, Wang G (2016) Glucose- and mannose-induced stomatal closure is mediated by ROS production, Ca2+ and water channel in Vicia faba. Physiologia Plantarum **156:** 252-261

Li Y, Xu S, Wang Z, He L, Xu K, Wang G (2018) Glucose triggers stomatal closure mediated by basal signaling through HXK1 and PYR/RCAR receptors in Arabidopsis. Journal of Experimental Botany **69:** 1471-1484

Lu P, Outlaw Jr WH, Smith BG, Freed GA (1997) A New Mechanism for the Regulation of Stomatal Aperture Size in Intact Leaves (Accumulation of Mesophyll-Derived Sucrose in the Guard-Cell Wall of Vicia faba). Plant Physiology **114:** 109-118

Lu P, Zhang SQ, Outlaw WH, Riddle KA (1995) Sucrose: a solute that accumulates in the guard-cell apoplast and guard-cell symplast of open stomata. FEBS Letters **362:** 180-184

Marco V, Hervé C, Giorgio G, Alexandre P, Irene P, Claudio L (2016) VvPIP2;4N aquaporin involvement in controlling leaf hydraulic capacitance and resistance in grapevine. Physiologia Plantarum **158:** 284-296

Martin-StPaul N, Delzon S, Cochard H (2017) Plant resistance to drought depends on timely stomatal closure. Ecology Letters **20:** 1437-1447

McAdam SAM, Brodribb TJ (2016) Linking turgor with ABA biosynthesis: implications for stomatal responses to vapor pressure deficit across land plants. Plant Physiology **171:** 2008-2016

Medeiros DB, Souza LP, Antunes WC, Araujo WL, Daloso DM, Fernie AR (2018) Sucrose breakdown within guard cells provides substrates for glycolysis and glutamine biosynthesis during light-induced stomatal opening. Plant Journal **94:** 583-594

Murray K, Conner MM (2009) Methods to quantify variable importance: implications for the analysis of noisy ecological data Ecology **90:** 348-355

Nardini A, Gortan E, Salleo S (2005a) Hydraulic efficiency of the leaf venation system in sun- and shade-adapted species. Functional Plant Biology **32:** 953-961

Nardini A, Salleo S (2003) Effects of the experimental blockage of the major veins on hydraulics and gas exchange of *Prunus laurocerasus* L. leaves. Journal of Experimental Botany **54:** 1213-1219

Nardini A, Salleo S (2005) Water stress-induced modifications of leaf hydraulic architecture in sunflower: co-ordination with gas exchange. Journal of Experimental Botany **56:** 3093-3101

Nardini A, Salleo S, Andri S (2005b) Circadian regulation of leaf hydraulic conductance in sunflower (*Helianthus annuus* L. cv Margot). Plant Cell and Environment **28:** 750-759

Nardini A, Tyree MT, Salleo S (2001) Xylem cavitation in the leaf of *Prunus laurocerasus* and its impact on leaf hydraulics. Plant Physiology **125:** 1700-1709

Nikinmaa E, Hölttä T, Hari P, Kolari P, Mäkelä A, Sevanto S, Vesala T (2013) Assimilate transport in phloem sets conditions for leaf gas exchange. Plant, Cell & Environment **36:** 655-669

Nolf M, Rosani A, Ganthaler A, Beikircher B, Mayr S (2016) Herb Hydraulics: Inter- and Intraspecific Variation in Three Ranunculus Species. Plant Physiology **170:** 2085–2094

Pantin F, Monnet F, Jannaud D, Costa JM, Renaud J, Muller B, Simonneau T, Genty B (2013) The dual effect of abscisic acid on stomata. New Phytologist **197:** 65-72

Petrie PR, Trought MCT, Howell GS (2000) Influence of leaf ageing, leaf area and crop load on photosynthesis, stomatal conductance and senescence of grapevine (Vitis vinifera L. cv. Pinot noir) leaves. Vitis **39:** 31-36

Pickard WF (1981) The ascent of sap in plants. Progress in Biophysics & Molecular Biology **37:** 181-229

Poorter H, Fiorani F, Pieruschka R, Wojciechowski T, Putten WH, Kleyer M, Schurr U, Postma J (2016) Pampered inside, pestered outside? Differences and similarities between plants growing in controlled conditions and in the field. New Phytologist **212:** 838-855

Pou A, Medrano H, Flexas J, Tyerman SD (2013) A putative role for TIP and PIP aquaporins in dynamics of leaf hydraulic and stomatal conductances in grapevine under water stress and re-watering. Plant Cell and Environment **36:** 828-843

Prado K, Boursiac Y, Tournaire-Roux C, Monneuse JM, Postaire O, Da Ines O, Schaffner AR, Hem S, Santoni V, Maurel C (2013) Regulation of Arabidopsis leaf hydraulics involves light-dependent phosphorylation of aquaporins in veins. Plant Cell **25:** 1029-1039

Rockwell FE, Gersony JT, Holbrook NM (2018) Where does Münch flow begin? Sucrose transport in the pre-phloem path. Current Opinion in Plant Biology **43:** 101-107

Rodriguez-Dominguez CM, Buckley TN, Egea G, de Cires A, Hernandez-Santana V, Martorell S, Diaz-Espejo A (2016) Most stomatal closure in woody species under moderate drought can be explained by stomatal responses to leaf turgor. Plant Cell and Environment **39:** 2014-2026

Rodriguez-Dominguez CM, Murphy MRC, Lucani C, Brodribb TJ (2018) Mapping xylem failure in disparate organs of whole plants reveals extreme resistance in olive roots. New Phytologist **218:** 1025-1035

Sack L, Cowan PD, Jaikumar N, Holbrook NM (2003) The 'hydrology' of leaves: co-ordination of structure and function in temperate woody species. Plant Cell and Environment **26:** 1343-1356

Sack L, Holbrook NM (2006) Leaf hydraulics. Annual Review of Plant Biology **57:** 361-381

Sack L, John GP, Buckley TN (2018) ABA accumulation in dehydrating leaves is associated with decline in cell volume, not turgor pressure. Plant Physiology **176:** 489-495

Sack L, Melcher PJ, Liu WH, Middleton E, Pardee T (2006) How strong is intracanopy leaf plasticity in temperate deciduous trees? American Journal of Botany **93:** 829-839

Sack L, Melcher PJ, Zwieniecki MA, Holbrook NM (2002) The hydraulic conductance of the angiosperm leaf lamina: a comparison of three measurement methods. Journal of Experimental Botany **53:** 2177-2184

Sack L, PrometheusWiki (2010) Leaf pressure-volume curve parameters *In*. PrometheusWiki http://www.publish.csiro.au/prometheuswiki/tiki-pagehistory.php?page=Leaf pressure-volume curve parameters&preview=10

Sack L, Scoffoni C (2013) Leaf venation: structure, function, development, evolution, ecology and applications in past, present and future. New Phytologist **198:** 938-1000

Sack L, Scoffoni C, PrometheusWiki c (2010) Minimum epidermal conductance (gmin a.k.a. cuticular conductance) *In*. PrometheusWiki http://www.publish.csiro.au/prometheuswiki/tiki-pagehistory.php?page=Minimum epidermal conductance (gmin%2C a.k.a. cuticular conductance)&preview=

Sack L, Streeter CM, Holbrook NM (2004) Hydraulic analysis of water flow through leaves of sugar maple and red oak. Plant Physiology **134:** 1824-1833

Sack L, Tyree MT, Holbrook NM (2005) Leaf hydraulic architecture correlates with regeneration irradiance in tropical rainforest trees. New Phytologist **167:** 403-413

Salleo S, Lo Gullo MA, Raimondo F, Nardini A (2001) Vulnerability to cavitation of leaf minor veins: any impact on leaf gas exchange? Plant Cell and Environment **24:** 851-859

Scoffoni C, Albuquerque C, Brodersen CR, Townes ST, John GP, Bartlett MK, Buckley TN, McElrone AJ, Sack L (2017a) Outside-xylem tissue vulnerability, not xylem embolism, controls leaf hydraulic decline with dehydration across diverse angiosperms. Plant Physiology **173** 1197-1210

Scoffoni C, Albuquerque C, Brodersen CR, Townes ST, John GP, Cochard H, Buckley TN, McElrone AJ, Sack L (2017b) Leaf vein xylem conduit diameter influences susceptibility to embolism and hydraulic decline. New Phytologist **213:** 1076–1092

Scoffoni C, Chatelet DS, Pasquet-Kok J, Rawls M, Donoghue MJ, Edwards EJ, L. S (2016) Hydraulic basis for the evolution of photosynthetic productivity. Nature Plants

Scoffoni C, Kunkle J, Pasquet-Kok J, Vuong C, Patel AJ, Montgomery RA, Givnish TJ, L. S (2015) Light-induced plasticity in leaf hydraulics, venation, anatomy and gas exchange in ecologically diverse Hawaiian lobeliads. New Phytologist **207:** 43-58

Scoffoni C, McKown AD, Rawls M, Sack L (2012) Dynamics of leaf hydraulic conductance with water status: quantification and analysis of species differences under steady-state. Journal of Experimental Botany **63:** 643-658

Scoffoni C, Pou A, Aasamaa K, Sack L (2008) The rapid light response of leaf hydraulic conductance: new evidence from two experimental methods. Plant Cell and Environment **31:** 1803-1812

Scoffoni C, Rawls M, McKown A, Cochard H, Sack L (2011) Decline of leaf hydraulic conductance with dehydration: relationship to leaf size and venation architecture. Plant Physiology **156:** 832-843

Scoffoni C, Sack L (2015) Are leaves “freewheelin'”? Testing for a Wheeler-type effect in leaf xylem hydraulic decline. Plant, Cell & Environment **38:** 534-543

Scoffoni C, Sack L (2017) The causes and consequences of leaf hydraulic decline with dehydration. Journal of Experimental Botany **68:** 4479-4496

Scoffoni C, Vuong C, Diep S, Cochard H, Sack L (2014) Leaf shrinkage with dehydration: coordination with hydraulic vulnerability and drought tolerance. Plant Physiology **164:** 1772-1788

Shatil-Cohen A, Attia Z, Moshelion M (2011) Bundle-sheath cell regulation of xylem-mesophyll water transport via aquaporins under drought stress: a target of xylem-borne ABA? Plant Journal **67:** 72-80

Skelton RP, Brodribb TJ, Choat B (2017) Casting light on xylem vulnerability in an herbaceous species reveals a lack of segmentation. New Phytologist **doi: 10.1111/nph.14450**

Stewart JJ, Polutchko SK, Demmig-Adams B, Adams WW (2018) Arabidopsis thaliana Ei-5: Minor Vein Architecture Adjustment Compensates for Low Vein Density in Support of Photosynthesis. Frontiers in Plant Science **9**

Sussmilch FC, Brodribb TJ, McAdam SAM (2017) Up-regulation of NCED3 and ABA biosynthesis occur within minutes of a decrease in leaf turgor but AHK1 is not required. Journal of Experimental Botany **68:** 2913-2918

Tixier A, Cochard H, Badel E, Dusotoit-Coucaud A, Jansen S, Herbette S (2013) *Arabidopsis thaliana* as a model species for xylem hydraulics: does size matter? Journal of Experimental Botany **64:** 2295-2305

Trifilo P, Raimondo F, Savi T, Lo Gullo MA, Nardini A (2016) The contribution of vascular and extra-vascular water pathways to drought-induced decline of leaf hydraulic conductance. Journal of Experimental Botany **67:** 5029-5039

Tyree MT, Davis SD, Cochard H (1994) Biophysical perspectives of xylem evolution: is there a tradeoff of hydraulic efficiency for vulnerability to dysfunction Iawa Journal **15:** 335-360

Tyree MT, Nardini A, Salleo S, Sack L, El Omari B (2005) The dependence of leaf hydraulic conductance on irradiance during HPFM measurements: any role for stomatal response? Journal of Experimental Botany **56:** 737-744

Van Houtte H, Vandesteene L, López-Galvis L, Lemmens L, Kissel E, Carpentier S, Feil R, Avonce N, Beeckman T, Lunn JE, Van Dijck P (2013) Overexpression of the Trehalase Gene AtTRE1 Leads to Increased Drought Stress Tolerance in Arabidopsis and Is Involved in Abscisic Acid-Induced Stomatal Closure. Plant Physiology **161:** 1158-1171

Voicu MC, Cooke JEK, Zwiazek JJ (2009) Aquaporin gene expression and apoplastic water flow in bur oak (Quercus macrocarpa) leaves in relation to the light response of leaf hydraulic conductance. Journal of Experimental Botany **60:** 4063-4075

Voicu MC, Zwiazek JJ, Tyree MT (2008) Light response of hydraulic conductance in bur oak (Quercus macrocarpa) leaves. Tree Physiology **28:** 1007-1015

Wang X, Du T, Huang J, Peng S, Xiong D (2018) Leaf Hydraulic Vulnerability Triggers the Decline in Stomatal and Mesophyll Conductance during drought in Rice (Oryza sativa). Journal of Experimental Botany**:** ery188-ery188

Weast RC (1974) Handbook of chemistry and physics. , 54th edn, Cleveland, OH: CRC Press.

Wright IJ, Reich PB, Westoby M, Ackerly DD, Baruch Z, Bongers F, Cavender-Bares J, Chapin T, Cornelissen JHC, Diemer M, Flexas J, Garnier E, Groom PK, Gulias J, Hikosaka K, Lamont BB, Lee T, Lee W, Lusk C, Midgley JJ, Navas ML, Niinemets U, Oleksyn J, Osada N, Poorter H, Poot P, Prior L, Pyankov VI, Roumet C, Thomas SC, Tjoelker MG, Veneklaas EJ, Villar R (2004) The worldwide leaf economics spectrum. Nature **428:** 821-827

Xiong D, Douthe C, Flexas J (2018) Differential coordination of stomatal conductance, mesophyll conductance, and leaf hydraulic conductance in response to changing light across species. Plant, Cell & Environment **41:** 436-450

Yang SD, Tyree MT (1993) Hydraulic resistance in *Acer saccharum* shoots and its influence on leaf water potential and transpiration. Tree Physiology **12:** 231-242

Zhang YJ, Rockwell FE, Graham AC, Alexander T, Holbrook NM (2016) Reversible leaf xylem collapse: a potential "circuit breaker" against cavitation. Plant Physiology **172:** 2261-2274

Buckley TN, John GP, Scoffoni C, Sack L (2017) The sites of evaporation within leaves. Plant Physiology **173:** 1763-1782

Cochard H, Nardini A, Coll L (2004) Hydraulic architecture of leaf blades: where is the main resistance? Plant Cell and Environment **27:** 1257-1267

Martin-StPaul N, Delzon S, Cochard H (2017) Plant resistance to drought depends on timely stomatal closure. Ecology Letters **20:** 1437-1447

Rodriguez-Dominguez CM, Buckley TN, Egea G, de Cires A, Hernandez-Santana V, Martorell S, Diaz-Espejo A (2016) Most stomatal closure in woody species under moderate drought can be explained by stomatal responses to leaf turgor. Plant Cell and Environment **39:** 2014-2026

Scoffoni C, Albuquerque C, Brodersen CR, Townes ST, John GP, Cochard H, Buckley TN, McElrone AJ, Sack L (2017) Leaf vein xylem conduit diameter influences susceptibility to embolism and hydraulic decline. New Phytologist **213:** 1076–1092

Zhang YJ, Rockwell FE, Graham AC, Alexander T, Holbrook NM (2016) Reversible leaf xylem collapse: a potential "circuit breaker" against cavitation. Plant Physiology **172:** 2261-2274

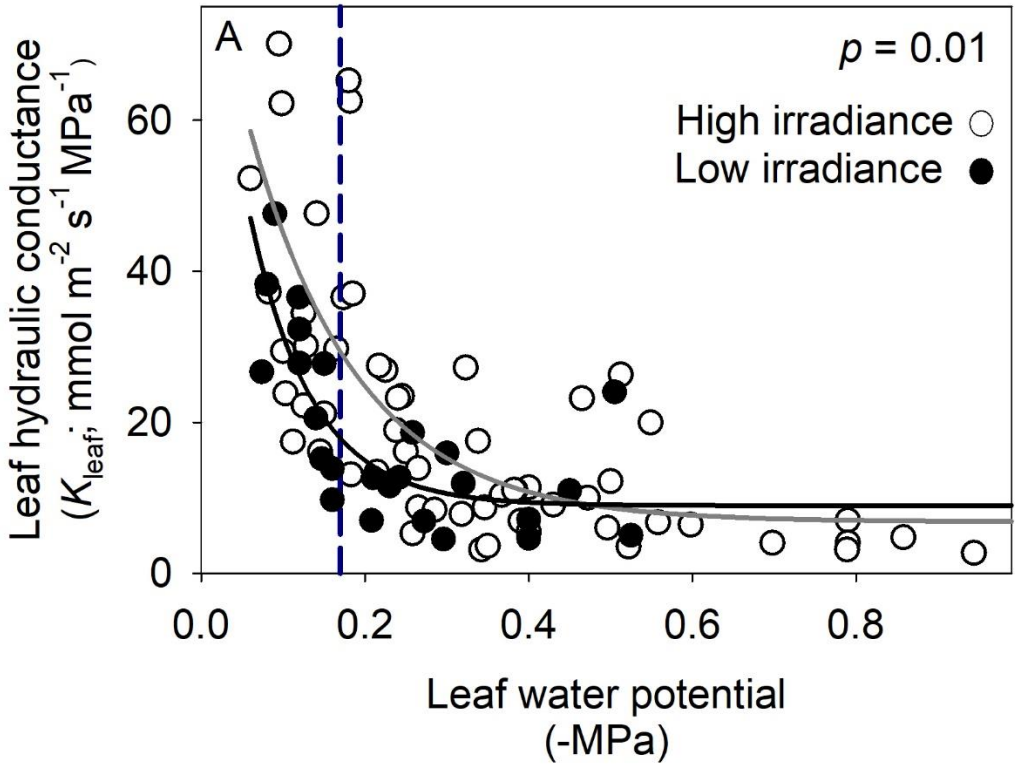

Figure 1. Decline of leaf hydraulic conductance (K_{leaf}) measured under high (>1000 µmol photons m^{-2} s^{-1}) or low (< 3 µmol photons m^{-2} s^{-1}) irradiance. The maximum likelihood function is shown for K_{leaf} vulnerability acclimated under high light ($K_{leaf} = 6.83 + 81.4\exp(-7.56 \times |\Psi_{leaf}|)$), and low light ($K_{leaf} = 8.98 + 84.2\exp(-13.2 \times |\Psi_{leaf}|)$). The dashed line respresents the water potential at 50% loss of K_{leaf} (similar in both treatments).

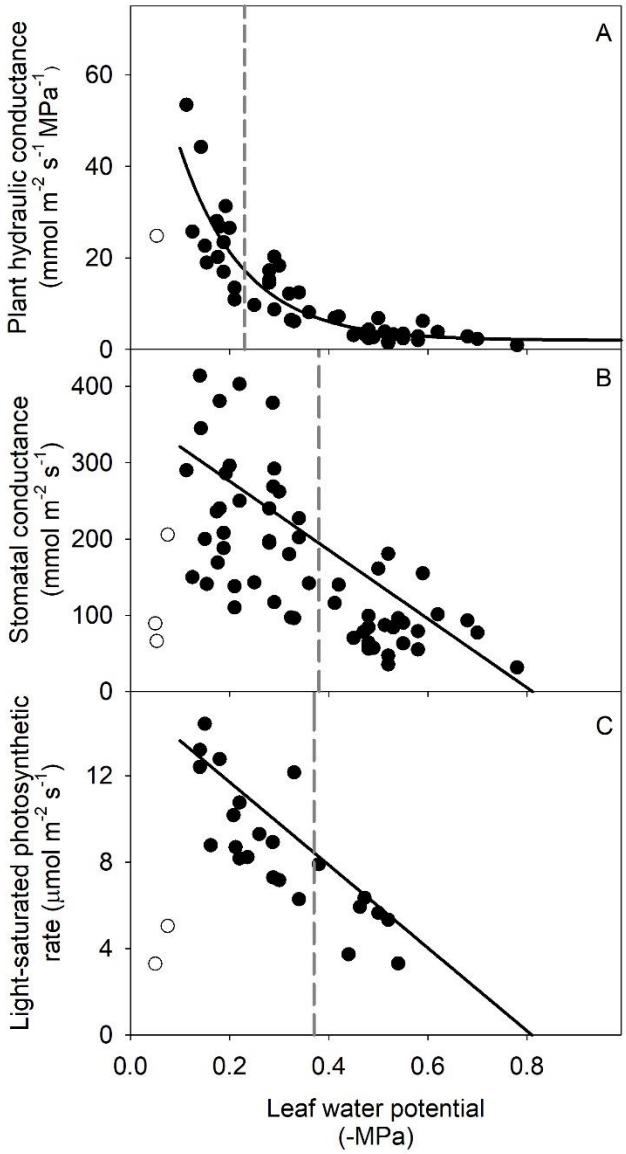

Figure 2. Plant hydraulic and gas exchange response to dehydration in Arabidopsis. Decline of the whole plant hydraulic conductance (K_{plant}; A), stomatal conductance (g_s; B) and light-saturated photosynthetic rate (A_{area}; C) with dehydration. Each point represents a different measured leaf. K_{plant} was obtained from the porometer data by dividing transpiration by leaf water potential (assuming soil water potential was at full saturation). The black fitted line in each pannel is the maximum likelihood function (exponential for $K_{\mathrm{plant}} = 2.0 + 91.1\exp(-7.75 \times |\Psi_{\mathrm{leaf}}|)$; linear for $g_{\mathrm{s}} = 339 - 451 \times |\Psi_{\mathrm{leaf}}|$, and $A_{\mathrm{area}} = 14.4 - 19.2 \times |\Psi_{\mathrm{leaf}}|$). The dotted grey line is the leaf water potential (Ψ_{leaf}) at 50% loss of maximum K_{plant}, g_s or A_{area}. Because trait values above -0.1 MPa were especially low (white circles), likely representing stomatal

closure at those high water potentials (see *Methods*), we did not include these points in the line fitting.

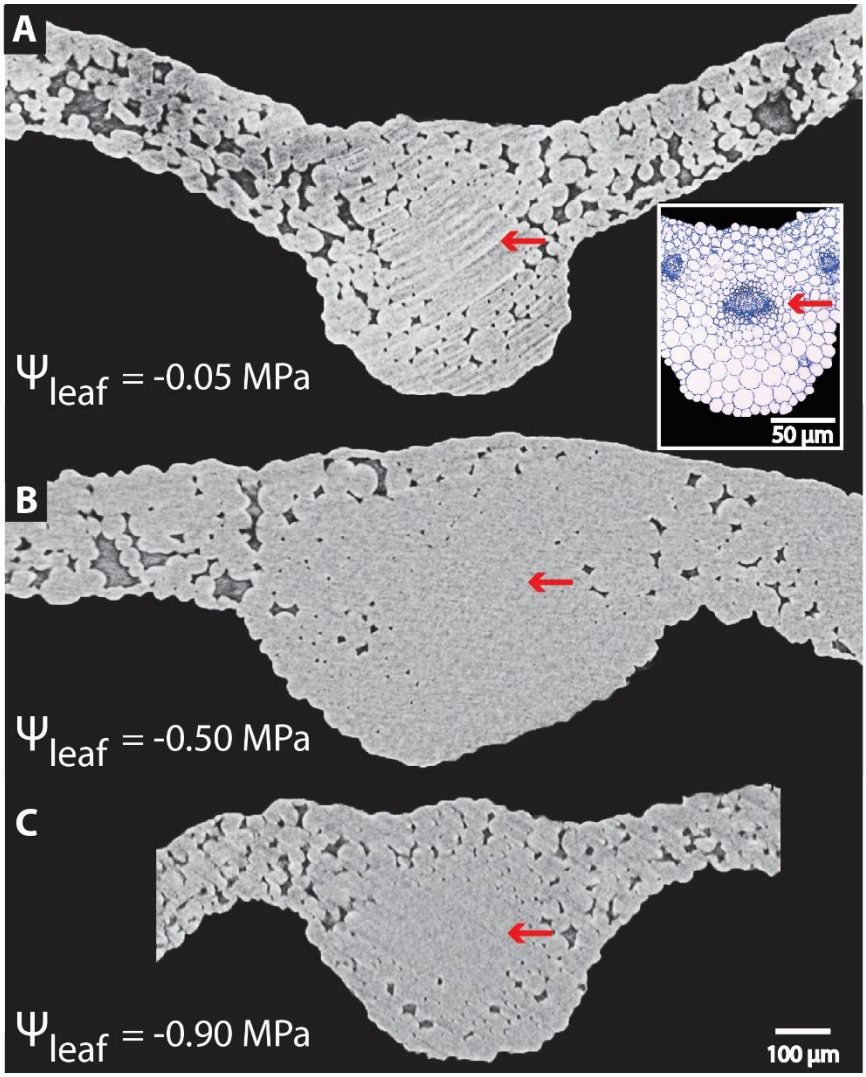

Figure 3. Lack of embolism observed in midrib conduits of *Arabidopsis thaliana* (Col-0) across levels of dehydration as revealed by in vivo images of leaf midribs subjected to progressive dehydration using micro-computed tomography (A-C). Water-filled cells appear in light grey in microCT. If air-filled (i.e., embolized) conduits were present, they would appear as black in the xylem portion of the midrib. There was no embolism, as shown in these images by the red arrows pointing at the entirely light grey midrib xylem. The leaf water potential (Ψ_{leaf}) has been provided for each image. The inset in (A) represents a leaf midrib cross-section imaged under light microscopy, with the red arrow pointing to the xylem tissue (dark blue conduits).

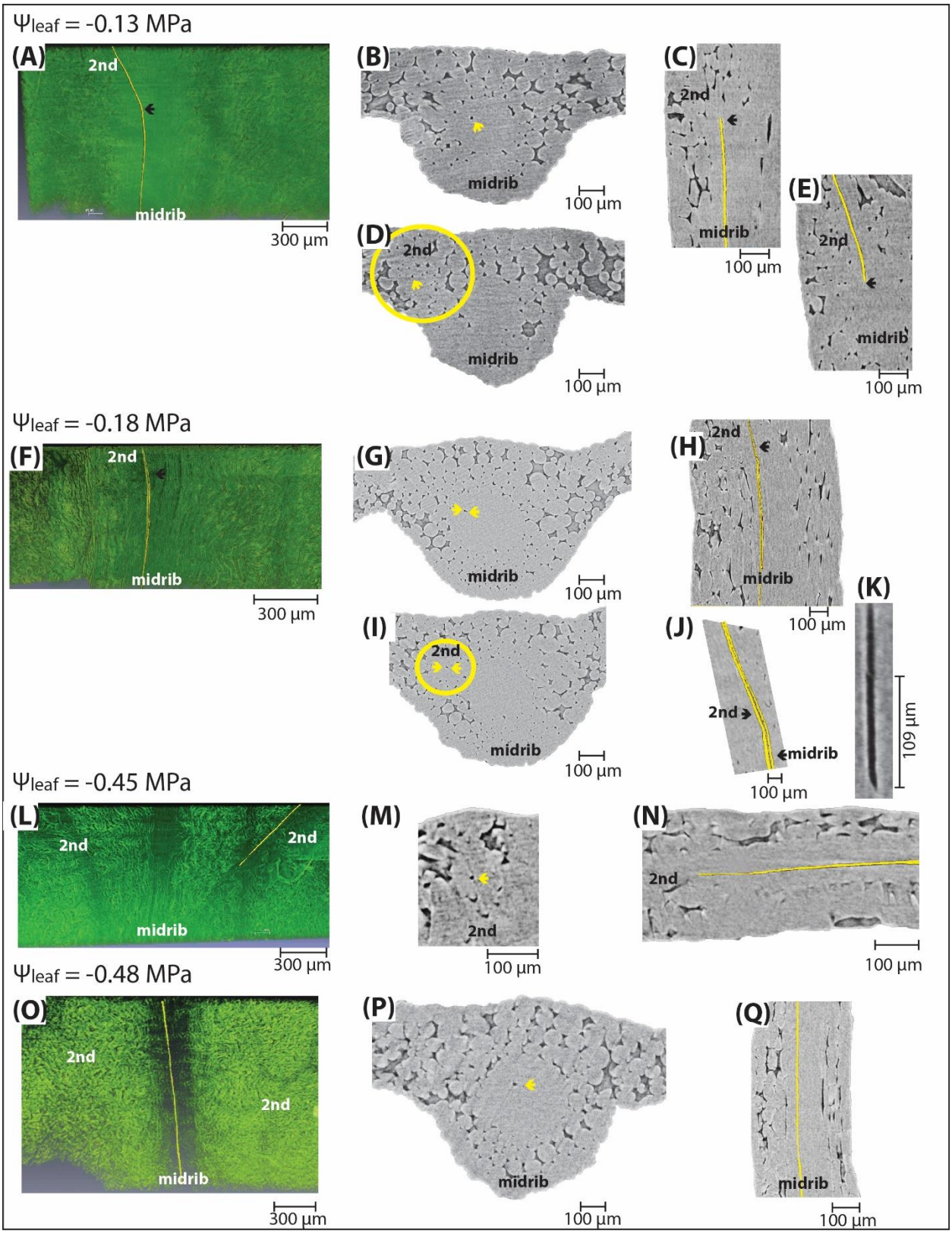

Figure 4. Rare embolisms were observed in a few individual leaves. In two samples, an embolized conduit was observed in the midrib; it continued into a secondary vein (A, F; the

embolized conduits are depicted in yellow). The embolized conduit in the midrib and secondary vein can be seen in cross-sections (B, D, G, I) and longitudinal sections of the microCT scan (C, E, H, J). The arrows point to the embolized conduit (appearing as black in the microCT image). Because of the two dimensionalities of these sections, embolism in the midrib and secondary vein might appear disconnected (C, E). Note that while the embolism was present in only one conduit per cross-sectional image, multiple conduits spanned the length of the midrib and secondary vein (as can be observed in K, where two conduits can be seen connected to one another). Most likely, a first conduit in the midrib embolized, and all the conduits directly connected to that one upstream embolized after. In one sample, an embolized conduit was observed isolated in the secondary vein (L-N), while in another sample, an embolized conduit was observed spanning the midrib length (O-Q).

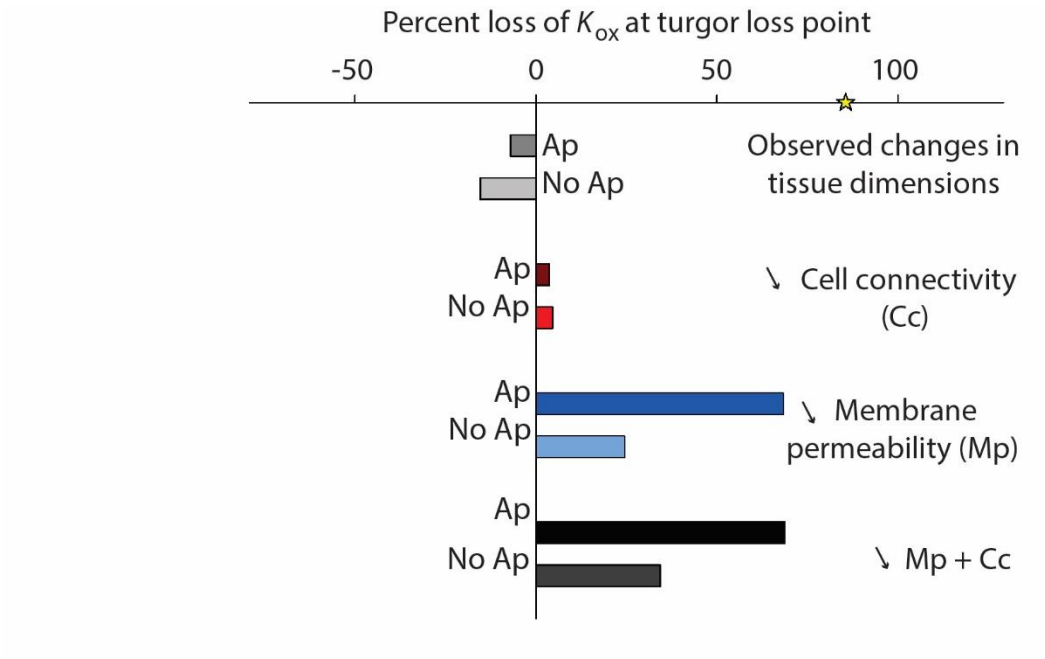

Figure 5. Results from simulations using a spatially explicit model of leaf outside-xylem water to test for potential drivers of the decline in K_{ox} in dehydrating leaves transport (MOFLO 2.0, see Table 1 and *Methods*). The K_{ox} was first computed based on the decline of observed cell size and air space alone (grey bars), which resulted in an increase in K_{ox} (negative percent loss of K_{ox}; mainly due to shortening of pathways from the veins to stomata). We then modelled K_{ox} decline according to three scenarios (though always including the effect of tissue dimensional changes): an 80% decline at -0.5MPa in (1) cell connectivity (red bars), (2) cell membrane permeability (blue bars), and (3) cell wall thickness (black bars). All simulations were run with (Ap; darker color) or without an apoplastic barrier (No Ap; lighter color) at the bundle sheath cells. The yellow star on the *x*-axis represents the % observed K_{leaf} decline at -0.5MPa (measured with the evaporative flux method, see *Methods*).

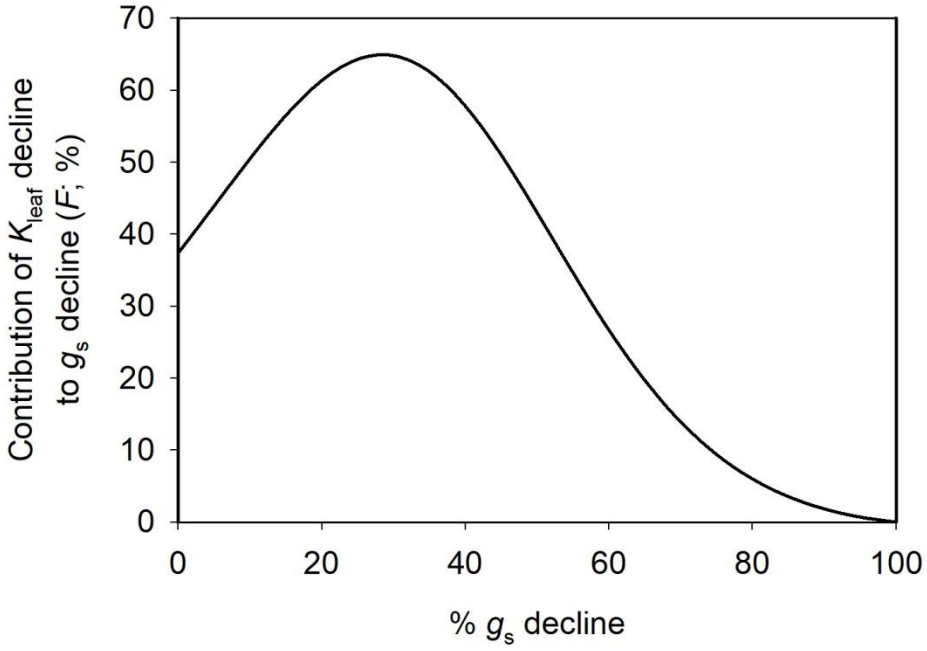

Figure 6. Model simulations mapping the contribution of the decline of leaf hydraulic conductance (K_{leaf}) decline to that of stomatal conductance (g_s) with dehydration (Table 1).

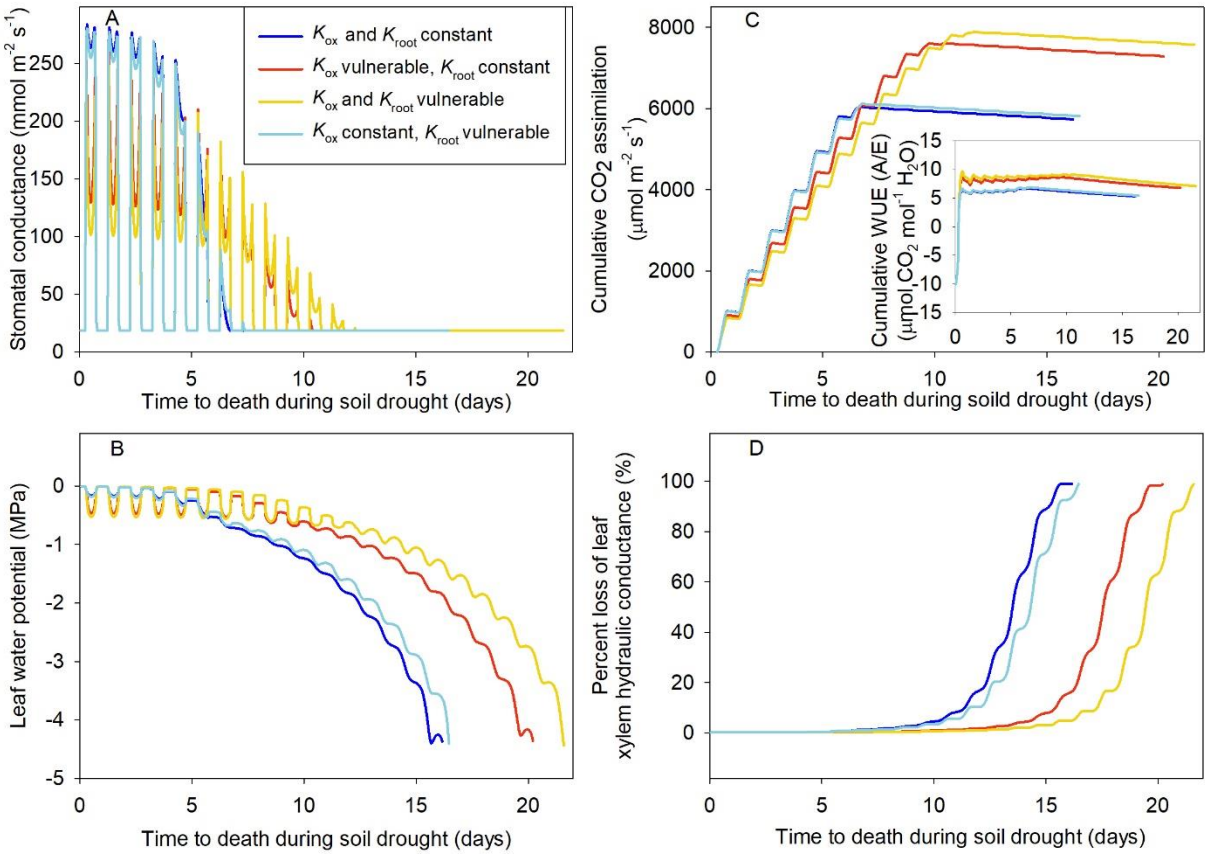

Figure 7. Daily simulated patterns of stomatal conductance (A), leaf water potential (B), cumulative CO_2 assimilation (C) and the percent loss of leaf xylem hydraulic conductance (D) during the progression of a simulated soil drought (SurEau Model, see Table 1 and *Methods*). Four scenarios were modelled: (1) both leaf hydraulic conductance (K_{leaf}) and root hydraulic conductance (K_{root}) were vulnerable to dehydration prior to turgor loss point (yellow lines), (2) K_{leaf} was vulnerable, but not K_{root} (red lines), 3) K_{root} was vulnerable, but not K_{leaf} (light blue lines), or (4) neither K_{leaf} nor K_{root} was vulnerable (dark blue lines). The inset in (C) shows cumulative water-use efficiency (WUE; calculated as cumulative CO_2 assimilation (A) over total transpiration rate (E)) over time. Scenarios including a vulnerable K_{leaf} showed leaves that showed highest water-use efficiency, cumulative CO_2 assimilation and survived longer under drought conditions.

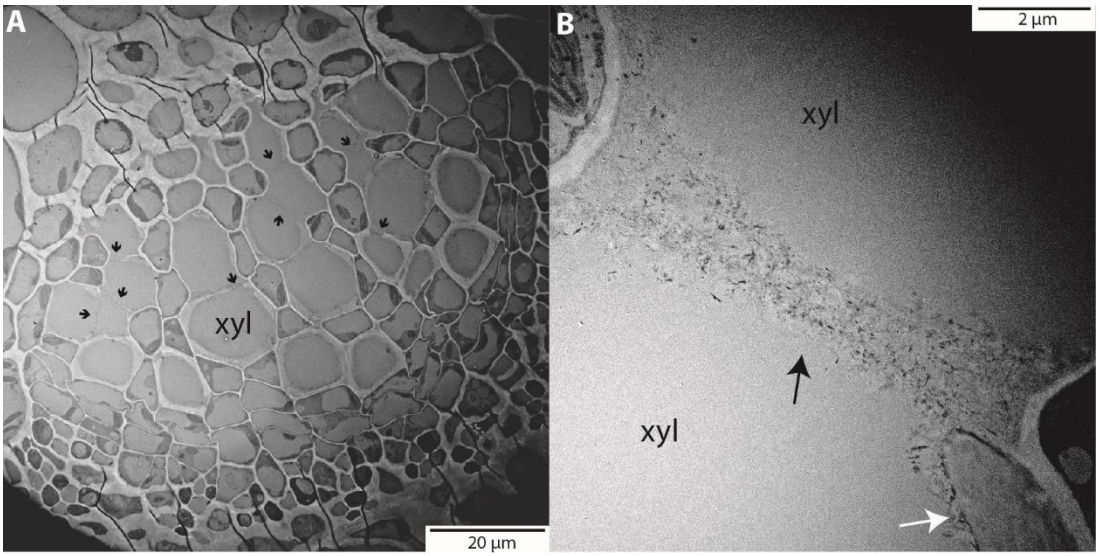

Figure 8. Transmitted-electron microscopy of *Arabidopsis thaliana* (Col-0) midrib cross-sections. In A, the entire xylem portion of the midrib can be seen. Black arrows point to the lack of secondary lignified wall around xylem conduits. These long primary wall sections can be observed in more detail in B. The white arrow points to a lignified portion of the secondary xylem wall. We hypothesize that the xylem resistance through these deeply helicoidal xylem conduits is greatly reduced, as unlignified primary cells effectively work as one large pit membrane.

Parsed Citations

Bartlett MK, Klein T, Jansen S, Choat B, L. S (2016) The correlations and sequence of plant stomatal, hydraulic, and wilting responses to drought. Proceedings of the National Academy of Sciences of the United States of America 113: 13098-13103
Pubmed: Author and Title
Google Scholar: Author Only Title Only Author and Title

Bartlett MK, Scoffoni C, Sack L (2012) The determinants of leaf turgor loss point and prediction of drought tolerance of species and biomes: a global meta-analysis. Ecology Letters 15: 393-405
Pubmed: Author and Title
Google Scholar: Author Only Title Only Author and Title

Ben Baaziz K, Lopez D, Rabot A, Combes D, Gousset A, Bouzid S, Cochard H, Sakr S, Venisse JS (2012) Light-mediated K-leaf induction and contribution of both the PIP1s and PIP2s aquaporins in five tree species: walnut (Juglans regia) case study. Tree Physiology 32: 423-434
Pubmed: Author and Title
Google Scholar: Author Only Title Only Author and Title

Blackman CJ, Brodribb TJ, Jordan GJ (2012) Leaf hydraulic vulnerability influences species' bioclimatic limits in a diverse group of woody angiosperms. Oecologia 168: 1-10
Pubmed: Author and Title
Google Scholar: Author Only Title Only Author and Title

Blackman CJ, Gleason SM, Chang Y, Cook AM, Laws C, Westoby M (2014) Leaf hydraulic vulnerability to drought is linked to site water availability across a broad range of species and climates. Annals of Botany 114: 435-440
Pubmed: Author and Title
Google Scholar: Author Only Title Only Author and Title

Bouche PS, Delzon S, Choat B, Badel E, Brodribb T, Burlett R, Cochard H, Charra-Vaskou K, Lavigne B, Shan L, Mayr S, Morris H, Torres-Ruiz JM, Zufferey V, Jansen S (2016) Are needles of Pinus pinaster more vulnerable to xylem embolism than branches? New insights from X-ray computed tomography. Plant, Cell & Environment 39: 860-870
Pubmed: Author and Title
Google Scholar: Author Only Title Only Author and Title

Brodersen CR, McElrone AJ, Choat B, Lee EF, Shackel KA, Matthews MA (2013) In Vivo Visualizations of Drought-Induced Embolism Spread in Vitis vinifera. Plant Physiology 161: 1820-1829
Pubmed: Author and Title
Google Scholar: Author Only Title Only Author and Title

Brodribb TJ, Bienaime D, Marmottant P (2016a) Revealing catastrophic failure of leaf networks under stress. Proceedings of the National Academy of Sciences of the United States of America 113: 4865-4869
Pubmed: Author and Title
Google Scholar: Author Only Title Only Author and Title

Brodribb TJ, Feild TS, Jordan GJ (2007) Leaf maximum photosynthetic rate and venation are linked by hydraulics. Plant Physiology 144: 1890-1898
Pubmed: Author and Title
Google Scholar: Author Only Title Only Author and Title

Brodribb TJ, Holbrook NM (2003a) Changes in leaf hydraulic conductance during leaf shedding in seasonally dry tropical forest. New Phytologist 158: 295-303
Pubmed: Author and Title
Google Scholar: Author Only Title Only Author and Title

Brodribb TJ, Holbrook NM (2003b) Stomatal closure during leaf dehydration, correlation with other leaf physiological traits. Plant Physiology 132: 2166-2173
Pubmed: Author and Title
Google Scholar: Author Only Title Only Author and Title

Brodribb TJ, Holbrook NM (2004) Stomatal protection against hydraulic failure: a comparison of coexisting ferns and angiosperms. New Phytologist 162: 663-670
Pubmed: Author and Title
Google Scholar: Author Only Title Only Author and Title

Brodribb TJ, Holbrook NM (2006) Declining hydraulic efficiency as transpiring leaves desiccate: two types of response. Plant Cell and Environment 29: 2205-2215
Pubmed: Author and Title
Google Scholar: Author Only Title Only Author and Title

Brodribb TJ, Holbrook NM (2007) Forced depression of leaf hydraulic conductance in situ: effects on the leaf gas exchange of forest trees. Functional Ecology 21: 705-712
Pubmed: Author and Title
Google Scholar: Author Only Title Only Author and Title

Scoffoni, C., Albuquerque, C., Bartlett, M., Brodersen, C. R., Jansen, S., McElrone, A. J., Sack, L. (2018). The Causes of Leaf Hydraulic Vulnerability and Its Influence on Gas Exchange in Arabidopsis thaliana. Plant Physiology, 178 (4), 1584-1601. , DOI : 10.1104/pp.18.00743

Brodribb TJ, Jordan GJ (2008) Internal coordination between hydraulics and stomatal control in leaves. Plant Cell and Environment 31: 1557-1564
Pubmed: Author and Title
Google Scholar: Author Only Title Only Author and Title

Brodribb TJ, Skelton RP, McAdam SAM, Bienaime D, Lucani CJ, Marmottant P (2016b) Visual quantification of embolism reveals leaf vulnerability to hydraulic failure. New Phytologist 209: 1403-1409
Pubmed: Author and Title
Google Scholar: Author Only Title Only Author and Title

Bucci SJ, Scholz FG, Goldstein G, Meinzer FC, Sternberg LDL (2003) Dynamic changes in hydraulic conductivity in petioles of two savanna tree species: factors and mechanisms contributing to the refilling of embolized vessels. Plant Cell and Environment 26: 1633-1645
Pubmed: Author and Title
Google Scholar: Author Only Title Only Author and Title

Buckley TN (2015) The contributions of apoplastic, symplastic and gas phase pathways for water transport outside the bundle sheath in leaves. Plant Cell and Environment 38: 7-22
Pubmed: Author and Title
Google Scholar: Author Only Title Only Author and Title

Buckley TN, John GP, Scoffoni C, Sack L (2015) How Does Leaf Anatomy Influence Water Transport outside the Xylem? Plant Physiology 168: 1616-1635
Pubmed: Author and Title
Google Scholar: Author Only Title Only Author and Title

Buckley TN, John GP, Scoffoni C, Sack L (2017a) The sites of evaporation within leaves. Plant Physiology 173: 1763-1782
Pubmed: Author and Title
Google Scholar: Author Only Title Only Author and Title

Buckley TN, Sack L, Farquhar GD (2017b) Optimal plant water economy. Plant, Cell & Environment 40: 881-896
Pubmed: Author and Title
Google Scholar: Author Only Title Only Author and Title

Burnham KP, Anderson DR (2002) Model selection and multimodel inference, 2nd ed. Springer, New York, New York, USA.
Pubmed: Author and Title
Google Scholar: Author Only Title Only Author and Title

Cairns Murphy MR, Jordan GJ, Brodribb TJ (2012) Differential leaf expansion can enable hydraulic acclimation to sun and shade. Plant, cell & environment 35
Pubmed: Author and Title
Google Scholar: Author Only Title Only Author and Title

Cardoso AA, Brodribb TJ, Lucani CJ, DaMatta FM, McAdam SAM (2018) Coordinated plasticity maintains hydraulic safety in sunflower leaves. Plant, Cell & Environment 0
Pubmed: Author and Title
Google Scholar: Author Only Title Only Author and Title

Caringella MA, Bongers FJ, Sack L (2015) Leaf hydraulic conductance varies with vein anatomy across Arabidopsis thaliana wild-type and leaf vein mutants. Plant Cell and Environment 38: 2735-2746
Pubmed: Author and Title
Google Scholar: Author Only Title Only Author and Title

Charra-Vaskou K, Badel E, Burlett R, Cochard H, Delzon S, Mayr S (2012) Hydraulic efficiency and safety of vascular and non-vascular components in Pinus pinaster leaves. Tree Physiology 32: 1161-1170
Pubmed: Author and Title
Google Scholar: Author Only Title Only Author and Title

Choat B, Badel E, Burlett R, Delzon S, Cochard H, Jansen S (2016) Non-invasive measurement of vulnerability to drought induced embolism by X-ray Microtomography. Plant Physiology 170: 273-282
Pubmed: Author and Title
Google Scholar: Author Only Title Only Author and Title

Choat B, Brodersen CR, McElrone AJ (2015) Synchrotron X-ray microtomography of xylem embolism in Sequoia sempervirens saplings during cycles of drought and recovery. New Phytologist 205: 1095-1105
Pubmed: Author and Title
Google Scholar: Author Only Title Only Author and Title

Choat B, Cobb AR, Jansen S (2008) Structure and function of bordered pits: new discoveries and impacts on whole-plant hydraulic function. New Phytologist 177: 608-625
Pubmed: Author and Title
Google Scholar: Author Only Title Only Author and Title

Cochard H, Froux F, Mayr FFS, Coutand C (2004a) Xylem wall collapse in water-stressed pine needles. Plant Physiology 134: 401-408
Pubmed: Author and Title

Google Scholar: Author Only Title Only Author and Title

Cochard H, Nardini A, Coll L (2004b) Hydraulic architecture of leaf blades: where is the main resistance? Plant Cell and Environment 27: 1257-1267
Pubmed: Author and Title
Google Scholar: Author Only Title Only Author and Title

Cochard H, Venisse JS, Barigah TS, Brunel N, Herbette S, Guilliot A, Tyree MT, Sakr S (2007) Putative role of aquaporins in variable hydraulic conductance of leaves in response to light. Plant Physiology 143: 122-133
Pubmed: Author and Title
Google Scholar: Author Only Title Only Author and Title

Cowan IR (1982) Water use and optimization of carbon assimilation. In Encyclopedia of plant physiology. 12B. Physiological plant ecology (eds Lange O. L., Nobel C.B., Osmond C.B. & Ziegler H.), Springer-Verlag, Berlin, pp 589–630
Pubmed: Author and Title
Google Scholar: Author Only Title Only Author and Title

Cuneo IF, Knipfer T, Brodersen C, McElrone AJ (2016) Mechanical failure of fine root cortical cells initiates plant hydraulic decline during drought. Plant Physiology doi:10.1104/pp.16.00923
Pubmed: Author and Title
Google Scholar: Author Only Title Only Author and Title

Delzon S, Cochard H (2014) Recent advances in tree hydraulics highlight the ecological significance of the hydraulic safety margin. New Phytologist 203: 355-358
Pubmed: Author and Title
Google Scholar: Author Only Title Only Author and Title

Flexas J, Scoffoni C, Gago J, Sack L (2013) Leaf mesophyll conductance and leaf hydraulic conductance: an introduction to their measurement and coordination. Journal of Experimental Botany 64: 3965-3981
Pubmed: Author and Title
Google Scholar: Author Only Title Only Author and Title

Gasco A, Nardini A, Salleo S (2004) Resistance to water flow through leaves of Coffea arabica is dominated by extra-vascular tissues. Functional Plant Biology 31: 1161-1168
Pubmed: Author and Title
Google Scholar: Author Only Title Only Author and Title

Grubb PJ (1998) A reassessment of the strategies of plants which cope with shortages of resources. Perspectives in Plant Ecology Evolution and Systematics 1: 3-31
Pubmed: Author and Title
Google Scholar: Author Only Title Only Author and Title

Guyot G, Scoffoni C, Sack L (2012) Combined impacts of irradiance and dehydration on leaf hydraulic conductance: insights into vulnerability and stomatal control. Plant, Cell & Environment 35: 857-871
Pubmed: Author and Title
Google Scholar: Author Only Title Only Author and Title

Hacke U, Sauter JJ (1996) Drought-induced xylem dysfunction in petioles, branches, and roots of Populus balsamifera L and Alnus glutinosa (L) Gaertn. Plant Physiology 111: 413-417
Pubmed: Author and Title
Google Scholar: Author Only Title Only Author and Title

Hacke UG, Sperry JS, Pittermann J (2000) Drought experience and cavitation resistance in six shrubs from the Great Basin, Utah. Basic and Applied Ecology 1: 31-41
Pubmed: Author and Title
Google Scholar: Author Only Title Only Author and Title

Hochberg U, Windt CW, Ponomarenko A, Zhang Y-J, Gersony J, Rockwell FE, Holbrook NM (2017) Stomatal closure, basal leaf embolism, and shedding protect the hydraulic integrity of grape stems. Plant Physiology 174: 764-775
Pubmed: Author and Title
Google Scholar: Author Only Title Only Author and Title

Hofäcker W (1978) Investigations on the photosynthesis of vines influence of defoliation, topping, girdling and removal of grapes Vitis 17: 10-22
Pubmed: Author and Title
Google Scholar: Author Only Title Only Author and Title

Jarzyniak KM, Jasiński M (2014) Membrane transporters and drought resistance – a complex issue. Frontiers in Plant Science 5: 687
Pubmed: Author and Title
Google Scholar: Author Only Title Only Author and Title

Javot H, Maurel C (2002) The role of aquaporins in root water uptake. Annals of Botany 90: 301-313
Pubmed: Author and Title
Google Scholar: Author Only Title Only Author and Title

Kang Y, Outlaw JWH, Fiore GB, Riddle KA (2007a) Guard cell apoplastic photosynthate accumulation corresponds to a phloem-loading mechanism. Journal of Experimental Botany 58: 4061-4070
Pubmed: Author and Title
Google Scholar: Author Only Title Only Author and Title

Kang Y, Outlaw WH, Andersen PC, Fiore GB (2007b) Guard-cell apoplastic sucrose concentration – a link between leaf photosynthesis and stomatal aperture size in the apoplastic phloem loader Vicia faba L. Plant, Cell & Environment 30: 551-558
Pubmed: Author and Title
Google Scholar: Author Only Title Only Author and Title

Kelly G, Moshelion M, David-Schwartz R, Halperin O, Wallach R, Attia Z, Belausov E, Granot D (2013) Hexokinase mediates stomatal closure. The Plant Journal 75: 977-988
Pubmed: Author and Title
Google Scholar: Author Only Title Only Author and Title

Kelly G, Sade N, Doron-Faigenboim A, Lerner S, Shatil-Cohen A, Yeselson Y, Egbaria A, Kottapalli J, Schaffer AA, Moshelion M, Granot D (2017) Sugar and hexokinase suppress expression of PIP aquaporins and reduce leaf hydraulics that preserves leaf water potential. The Plant Journal 91: 325-339
Pubmed: Author and Title
Google Scholar: Author Only Title Only Author and Title

Kolb KJ, Sperry JS, Lamont BB (1996) A method for measuring xylem hydraulic conductance and embolism in entire root and shoot systems. Journal of Experimental Botany 47: 1805-1810
Pubmed: Author and Title
Google Scholar: Author Only Title Only Author and Title

Koornneef M, Alonso-Blanco C, Vreugdenhil D (2004) Naturally occurring genetic variation in Arabidopsis thaliana. Annual Review of Plant Biology 55: 141-172
Pubmed: Author and Title
Google Scholar: Author Only Title Only Author and Title

Körner C (2015) Paradigm shift in plant growth control. Current Opinion in Plant Biology 25: 107-114
Pubmed: Author and Title
Google Scholar: Author Only Title Only Author and Title

Laur J, Hacke UG (2014a) Exploring Picea glauca aquaporins in the context of needle water uptake and xylem refilling. New Phytologist 203: 388-400
Pubmed: Author and Title
Google Scholar: Author Only Title Only Author and Title

Laur J, Hacke UG (2014b) The role of water channel proteins in facilitating recovery of leaf hydraulic conductance from water stress in Populus trichocarpa. Plos One 9
Pubmed: Author and Title
Google Scholar: Author Only Title Only Author and Title

Levin M, Lemcoff JH, Cohen S, Kapulnik Y (2007) Low air humidity increases leaf-specific hydraulic conductance of Arabidopsis thaliana (L.) Heynh (Brassicaceae). Journal of Experimental Botany 58: 3711-3718
Pubmed: Author and Title
Google Scholar: Author Only Title Only Author and Title

Li Y, Xu S, Gao J, Pan S, Wang G (2016) Glucose- and mannose-induced stomatal closure is mediated by ROS production, Ca2+ and water channel in Vicia faba. Physiologia Plantarum 156: 252-261
Pubmed: Author and Title
Google Scholar: Author Only Title Only Author and Title

Li Y, Xu S, Wang Z, He L, Xu K, Wang G (2018) Glucose triggers stomatal closure mediated by basal signaling through HXK1 and PYR/RCAR receptors in Arabidopsis. Journal of Experimental Botany 69: 1471-1484
Pubmed: Author and Title
Google Scholar: Author Only Title Only Author and Title

Lu P, Outlaw Jr WH, Smith BG, Freed GA (1997) A New Mechanism for the Regulation of Stomatal Aperture Size in Intact Leaves (Accumulation of Mesophyll-Derived Sucrose in the Guard-Cell Wall of Vicia faba). Plant Physiology 114: 109-118
Pubmed: Author and Title
Google Scholar: Author Only Title Only Author and Title

Lu P, Zhang SQ, Outlaw WH, Riddle KA (1995) Sucrose: a solute that accumulates in the guard-cell apoplast and guard-cell symplast of open stomata. FEBS Letters 362: 180-184
Pubmed: Author and Title
Google Scholar: Author Only Title Only Author and Title

Marco V, Hervé C, Giorgio G, Alexandre P, Irene P, Claudio L (2016) VvPIP2;4N aquaporin involvement in controlling leaf hydraulic capacitance and resistance in grapevine. Physiologia Plantarum 158: 284-296
Pubmed: Author and Title
Google Scholar: Author Only Title Only Author and Title

Martin-StPaul N, Delzon S, Cochard H (2017) Plant resistance to drought depends on timely stomatal closure. Ecology Letters 20: 1437-1447
Pubmed: Author and Title
Google Scholar: Author Only Title Only Author and Title

McAdam SAM, Brodribb TJ (2016) Linking turgor with ABA biosynthesis: implications for stomatal responses to vapor pressure deficit across land plants. Plant Physiology 171: 2008-2016
Pubmed: Author and Title
Google Scholar: Author Only Title Only Author and Title

Medeiros DB, Souza LP, Antunes WC, Araujo WL, Daloso DM, Fernie AR (2018) Sucrose breakdown within guard cells provides substrates for glycolysis and glutamine biosynthesis during light-induced stomatal opening. Plant Journal 94: 583-594
Pubmed: Author and Title
Google Scholar: Author Only Title Only Author and Title

Murray K, Conner MM (2009) Methods to quantify variable importance: implications for the analysis of noisy ecological data Ecology 90: 348-355
Pubmed: Author and Title
Google Scholar: Author Only Title Only Author and Title

Nardini A, Gortan E, Salleo S (2005a) Hydraulic efficiency of the leaf venation system in sun- and shade-adapted species. Functional Plant Biology 32: 953-961
Pubmed: Author and Title
Google Scholar: Author Only Title Only Author and Title

Nardini A, Salleo S (2003) Effects of the experimental blockage of the major veins on hydraulics and gas exchange of Prunus laurocerasus L. leaves. Journal of Experimental Botany 54: 1213-1219
Pubmed: Author and Title
Google Scholar: Author Only Title Only Author and Title

Nardini A, Salleo S (2005) Water stress-induced modifications of leaf hydraulic architecture in sunflower: co-ordination with gas exchange. Journal of Experimental Botany 56: 3093-3101
Pubmed: Author and Title
Google Scholar: Author Only Title Only Author and Title

Nardini A, Salleo S, Andri S (2005b) Circadian regulation of leaf hydraulic conductance in sunflower (Helianthus annuus L. cv Margot). Plant Cell and Environment 28: 750-759
Pubmed: Author and Title
Google Scholar: Author Only Title Only Author and Title

Nardini A, Tyree MT, Salleo S (2001) Xylem cavitation in the leaf of Prunus laurocerasus and its impact on leaf hydraulics. Plant Physiology 125: 1700-1709
Pubmed: Author and Title
Google Scholar: Author Only Title Only Author and Title

Nikinmaa E, Hölttä T, Hari P, Kolari P, Mäkelä A, Sevanto S, Vesala T (2013) Assimilate transport in phloem sets conditions for leaf gas exchange. Plant, Cell & Environment 36: 655-669
Pubmed: Author and Title
Google Scholar: Author Only Title Only Author and Title

Nolf M, Rosani A, Ganthaler A, Beikircher B, Mayr S (2016) Herb Hydraulics: Inter- and Intraspecific Variation in Three Ranunculus Species. Plant Physiology 170: 2085–2094
Pubmed: Author and Title
Google Scholar: Author Only Title Only Author and Title

Pantin F, Monnet F, Jannaud D, Costa JM, Renaud J, Muller B, Simonneau T, Genty B (2013) The dual effect of abscisic acid on stomata. New Phytologist 197: 65-72
Pubmed: Author and Title
Google Scholar: Author Only Title Only Author and Title

Petrie PR, Trought MCT, Howell GS (2000) Influence of leaf ageing, leaf area and crop load on photosynthesis, stomatal conductance and senescence of grapevine (Vitis vinifera L. cv. Pinot noir) leaves. Vitis 39: 31-36
Pubmed: Author and Title
Google Scholar: Author Only Title Only Author and Title

Pickard WF (1981) The ascent of sap in plants. Progress in Biophysics & Molecular Biology 37: 181-229
Pubmed: Author and Title
Google Scholar: Author Only Title Only Author and Title

Poorter H, Fiorani F, Pieruschka R, Wojciechowski T, Putten WH, Kleyer M, Schurr U, Postma J (2016) Pampered inside, pestered outside? Differences and similarities between plants growing in controlled conditions and in the field. New Phytologist 212: 838-855
Pubmed: Author and Title
Google Scholar: Author Only Title Only Author and Title

Pou A, Medrano H, Flexas J, Tyerman SD (2013) A putative role for TIP and PIP aquaporins in dynamics of leaf hydraulic and stomatal

conductances in grapevine under water stress and re-watering. Plant Cell and Environment 36: 828-843
Pubmed: Author and Title
Google Scholar: Author Only Title Only Author and Title

Prado K, Boursiac Y, Tournaire-Roux C, Monneuse JM, Postaire O, Da Ines O, Schaffner AR, Hem S, Santoni V, Maurel C (2013) Regulation of Arabidopsis leaf hydraulics involves light-dependent phosphorylation of aquaporins in veins. Plant Cell 25: 1029-1039
Pubmed: Author and Title
Google Scholar: Author Only Title Only Author and Title

Rockwell FE, Gersony JT, Holbrook NM (2018) Where does Münch flow begin? Sucrose transport in the pre-phloem path. Current Opinion in Plant Biology 43: 101-107
Pubmed: Author and Title
Google Scholar: Author Only Title Only Author and Title

Rodriguez-Dominguez CM, Buckley TN, Egea G, de Cires A, Hernandez-Santana V, Martorell S, Diaz-Espejo A (2016) Most stomatal closure in woody species under moderate drought can be explained by stomatal responses to leaf turgor. Plant Cell and Environment 39: 2014-2026
Pubmed: Author and Title
Google Scholar: Author Only Title Only Author and Title

Rodriguez-Dominguez CM, Murphy MRC, Lucani C, Brodribb TJ (2018) Mapping xylem failure in disparate organs of whole plants reveals extreme resistance in olive roots. New Phytologist 218: 1025-1035
Pubmed: Author and Title
Google Scholar: Author Only Title Only Author and Title

Sack L, Cowan PD, Jaikumar N, Holbrook NM (2003) The 'hydrology' of leaves: co-ordination of structure and function in temperate woody species. Plant Cell and Environment 26: 1343-1356
Pubmed: Author and Title
Google Scholar: Author Only Title Only Author and Title

Sack L, Holbrook NM (2006) Leaf hydraulics. Annual Review of Plant Biology 57: 361-381
Pubmed: Author and Title
Google Scholar: Author Only Title Only Author and Title

Sack L, John GP, Buckley TN (2018) ABA accumulation in dehydrating leaves is associated with decline in cell volume, not turgor pressure. Plant Physiology 176: 489-495
Pubmed: Author and Title
Google Scholar: Author Only Title Only Author and Title

Sack L, Melcher PJ, Liu WH, Middleton E, Pardee T (2006) How strong is intracanopy leaf plasticity in temperate deciduous trees? American Journal of Botany 93: 829-839
Pubmed: Author and Title
Google Scholar: Author Only Title Only Author and Title

Sack L, Melcher PJ, Zwieniecki MA, Holbrook NM (2002) The hydraulic conductance of the angiosperm leaf lamina: a comparison of three measurement methods. Journal of Experimental Botany 53: 2177-2184
Pubmed: Author and Title
Google Scholar: Author Only Title Only Author and Title

Sack L, PrometheusWiki (2010) Leaf pressure-volume curve parameters In. PrometheusWiki http://www.publish.csiro.au/prometheuswiki/tiki-pagehistory.php?page=Leaf pressure-volume curve parameters&preview=10
Pubmed: Author and Title
Google Scholar: Author Only Title Only Author and Title

Sack L, Scoffoni C (2013) Leaf venation: structure, function, development, evolution, ecology and applications in past, present and future. New Phytologist 198: 938-1000
Pubmed: Author and Title
Google Scholar: Author Only Title Only Author and Title

Sack L, Scoffoni C, PrometheusWiki c (2010) Minimum epidermal conductance (gmin a.k.a. cuticular conductance) In. PrometheusWiki http://www.publish.csiro.au/prometheuswiki/tiki-pagehistory.php?page=Minimum epidermal conductance (gmin%2C a.k.a. cuticular conductance)&preview=
Pubmed: Author and Title
Google Scholar: Author Only Title Only Author and Title

Sack L, Streeter CM, Holbrook NM (2004) Hydraulic analysis of water flow through leaves of sugar maple and red oak. Plant Physiology 134: 1824-1833
Pubmed: Author and Title
Google Scholar: Author Only Title Only Author and Title

Sack L, Tyree MT, Holbrook NM (2005) Leaf hydraulic architecture correlates with regeneration irradiance in tropical rainforest trees. New Phytologist 167: 403-413
Pubmed: Author and Title
Google Scholar: Author Only Title Only Author and Title

Salleo S, Lo Gullo MA, Raimondo F, Nardini A (2001) Vulnerability to cavitation of leaf minor veins: any impact on leaf gas exchange? Plant Cell and Environment 24: 851-859
Pubmed: Author and Title
Google Scholar: Author Only Title Only Author and Title

Scoffoni C, Albuquerque C, Brodersen CR, Townes ST, John GP, Bartlett MK, Buckley TN, McElrone AJ, Sack L (2017a) Outside-xylem tissue vulnerability, not xylem embolism, controls leaf hydraulic decline with dehydration across diverse angiosperms. Plant Physiology 173 1197-1210
Pubmed: Author and Title
Google Scholar: Author Only Title Only Author and Title

Scoffoni C, Albuquerque C, Brodersen CR, Townes ST, John GP, Cochard H, Buckley TN, McElrone AJ, Sack L (2017b) Leaf vein xylem conduit diameter influences susceptibility to embolism and hydraulic decline. New Phytologist 213: 1076–1092
Pubmed: Author and Title
Google Scholar: Author Only Title Only Author and Title

Scoffoni C, Chatelet DS, Pasquet-Kok J, Rawls M, Donoghue MJ, Edwards EJ, L. S (2016) Hydraulic basis for the evolution of photosynthetic productivity. Nature Plants
Pubmed: Author and Title
Google Scholar: Author Only Title Only Author and Title

Scoffoni C, Kunkle J, Pasquet-Kok J, Vuong C, Patel AJ, Montgomery RA, Givnish TJ, L. S (2015) Light-induced plasticity in leaf hydraulics, venation, anatomy and gas exchange in ecologically diverse Hawaiian lobeliads. New Phytologist 207: 43-58
Pubmed: Author and Title
Google Scholar: Author Only Title Only Author and Title

Scoffoni C, McKown AD, Rawls M, Sack L (2012) Dynamics of leaf hydraulic conductance with water status: quantification and analysis of species differences under steady-state. Journal of Experimental Botany 63: 643-658
Pubmed: Author and Title
Google Scholar: Author Only Title Only Author and Title

Scoffoni C, Pou A, Aasamaa K, Sack L (2008) The rapid light response of leaf hydraulic conductance: new evidence from two experimental methods. Plant Cell and Environment 31: 1803-1812
Pubmed: Author and Title
Google Scholar: Author Only Title Only Author and Title

Scoffoni C, Rawls M, McKown A, Cochard H, Sack L (2011) Decline of leaf hydraulic conductance with dehydration: relationship to leaf size and venation architecture. Plant Physiology 156: 832-843
Pubmed: Author and Title
Google Scholar: Author Only Title Only Author and Title

Scoffoni C, Sack L (2015) Are leaves "freewheelin'"? Testing for a Wheeler-type effect in leaf xylem hydraulic decline. Plant, Cell & Environment 38: 534-543
Pubmed: Author and Title
Google Scholar: Author Only Title Only Author and Title

Scoffoni C, Sack L (2017) The causes and consequences of leaf hydraulic decline with dehydration. Journal of Experimental Botany 68: 4479-4496
Pubmed: Author and Title
Google Scholar: Author Only Title Only Author and Title

Scoffoni C, Vuong C, Diep S, Cochard H, Sack L (2014) Leaf shrinkage with dehydration: coordination with hydraulic vulnerability and drought tolerance. Plant Physiology 164: 1772-1788
Pubmed: Author and Title
Google Scholar: Author Only Title Only Author and Title

Shatil-Cohen A, Attia Z, Moshelion M (2011) Bundle-sheath cell regulation of xylem-mesophyll water transport via aquaporins under drought stress: a target of xylem-borne ABA? Plant Journal 67: 72-80
Pubmed: Author and Title
Google Scholar: Author Only Title Only Author and Title

Skelton RP, Brodribb TJ, Choat B (2017) Casting light on xylem vulnerability in an herbaceous species reveals a lack of segmentation. New Phytologist doi: 10.1111/nph.14450
Pubmed: Author and Title
Google Scholar: Author Only Title Only Author and Title

Stewart JJ, Polutchko SK, Demmig-Adams B, Adams WW (2018) Arabidopsis thaliana Ei-5: Minor Vein Architecture Adjustment Compensates for Low Vein Density in Support of Photosynthesis. Frontiers in Plant Science 9
Pubmed: Author and Title
Google Scholar: Author Only Title Only Author and Title

Sussmilch FC, Brodribb TJ, McAdam SAM (2017) Up-regulation of NCED3 and ABA biosynthesis occur within minutes of a decrease in leaf turgor but AHK1 is not required. Journal of Experimental Botany 68: 2913-2918
Pubmed: Author and Title
Google Scholar: Author Only Title Only Author and Title

Tixier A, Cochard H, Badel E, Dusotoit-Coucaud A, Jansen S, Herbette S (2013) Arabidopsis thaliana as a model species for xylem hydraulics: does size matter? Journal of Experimental Botany 64: 2295-2305
Pubmed: Author and Title
Google Scholar: Author Only Title Only Author and Title

Trifilo P, Raimondo F, Savi T, Lo Gullo MA, Nardini A (2016) The contribution of vascular and extra-vascular water pathways to drought-induced decline of leaf hydraulic conductance. Journal of Experimental Botany 67: 5029-5039
Pubmed: Author and Title
Google Scholar: Author Only Title Only Author and Title

Tyree MT, Davis SD, Cochard H (1994) Biophysical perspectives of xylem evolution: is there a tradeoff of hydraulic efficiency for vulnerability to dysfunction Iawa Journal 15: 335-360
Pubmed: Author and Title
Google Scholar: Author Only Title Only Author and Title

Tyree MT, Nardini A, Salleo S, Sack L, El Omari B (2005) The dependence of leaf hydraulic conductance on irradiance during HPFM measurements: any role for stomatal response? Journal of Experimental Botany 56: 737-744
Pubmed: Author and Title
Google Scholar: Author Only Title Only Author and Title

Van Houtte H, Vandesteene L, López-Galvis L, Lemmens L, Kissel E, Carpentier S, Feil R, Avonce N, Beeckman T, Lunn JE, Van Dijck P (2013) Overexpression of the Trehalase Gene AtTRE1 Leads to Increased Drought Stress Tolerance in Arabidopsis and Is Involved in Abscisic Acid-Induced Stomatal Closure. Plant Physiology 161: 1158-1171
Pubmed: Author and Title
Google Scholar: Author Only Title Only Author and Title

Voicu MC, Cooke JEK, Zwiazek JJ (2009) Aquaporin gene expression and apoplastic water flow in bur oak (Quercus macrocarpa) leaves in relation to the light response of leaf hydraulic conductance. Journal of Experimental Botany 60: 4063-4075
Pubmed: Author and Title
Google Scholar: Author Only Title Only Author and Title

Voicu MC, Zwiazek JJ, Tyree MT (2008) Light response of hydraulic conductance in bur oak (Quercus macrocarpa) leaves. Tree Physiology 28: 1007-1015
Pubmed: Author and Title
Google Scholar: Author Only Title Only Author and Title

Wang X, Du T, Huang J, Peng S, Xiong D (2018) Leaf Hydraulic Vulnerability Triggers the Decline in Stomatal and Mesophyll Conductance during drought in Rice (Oryza sativa). Journal of Experimental Botany: ery188-ery188
Pubmed: Author and Title
Google Scholar: Author Only Title Only Author and Title

Weast RC (1974) Handbook of chemistry and physics. , 54th edn, Cleveland, OH: CRC Press.

Wright IJ, Reich PB, Westoby M, Ackerly DD, Baruch Z, Bongers F, Cavender-Bares J, Chapin T, Cornelissen JHC, Diemer M, Flexas J, Garnier E, Groom PK, Gulias J, Hikosaka K, Lamont BB, Lee T, Lee W, Lusk C, Midgley JJ, Navas ML, Niinemets U, Oleksyn J, Osada N, Poorter H, Poot P, Prior L, Pyankov VI, Roumet C, Thomas SC, Tjoelker MG, Veneklaas EJ, Villar R (2004) The worldwide leaf economics spectrum. Nature 428: 821-827
Pubmed: Author and Title
Google Scholar: Author Only Title Only Author and Title

Xiong D, Douthe C, Flexas J (2018) Differential coordination of stomatal conductance, mesophyll conductance, and leaf hydraulic conductance in response to changing light across species. Plant, Cell & Environment 41: 436-450
Pubmed: Author and Title
Google Scholar: Author Only Title Only Author and Title

Yang SD, Tyree MT (1993) Hydraulic resistance in Acer saccharum shoots and its influence on leaf water potential and transpiration. Tree Physiology 12: 231-242
Pubmed: Author and Title
Google Scholar: Author Only Title Only Author and Title

Zhang YJ, Rockwell FE, Graham AC, Alexander T, Holbrook NM (2016) Reversible leaf xylem collapse: a potential "circuit breaker" against cavitation. Plant Physiology 172: 2261-2274
Pubmed: Author and Title
Google Scholar: Author Only Title Only Author and Title

Buckley TN, John GP, Scoffoni C, Sack L (2017) The sites of evaporation within leaves. Plant Physiology 173: 1763-1782
Pubmed: Author and Title
Google Scholar: Author Only Title Only Author and Title

Cochard H, Nardini A, Coll L (2004) Hydraulic architecture of leaf blades: where is the main resistance? Plant Cell and Environment 27: 1257-1267
Pubmed: Author and Title
Google Scholar: Author Only Title Only Author and Title

Martin-StPaul N, Delzon S, Cochard H (2017) Plant resistance to drought depends on timely stomatal closure. Ecology Letters 20: 1437-1447
Pubmed: Author and Title
Google Scholar: Author Only Title Only Author and Title

Rodriguez-Dominguez CM, Buckley TN, Egea G, de Cires A, Hernandez-Santana V, Martorell S, Diaz-Espejo A (2016) Most stomatal closure in woody species under moderate drought can be explained by stomatal responses to leaf turgor. Plant Cell and Environment 39: 2014-2026
Pubmed: Author and Title
Google Scholar: Author Only Title Only Author and Title

Scoffoni C, Albuquerque C, Brodersen CR, Townes ST, John GP, Cochard H, Buckley TN, McElrone AJ, Sack L (2017) Leaf vein xylem conduit diameter influences susceptibility to embolism and hydraulic decline. New Phytologist 213: 1076–1092
Pubmed: Author and Title
Google Scholar: Author Only Title Only Author and Title

Zhang YJ, Rockwell FE, Graham AC, Alexander T, Holbrook NM (2016) Reversible leaf xylem collapse: a potential "circuit breaker" against cavitation. Plant Physiology 172: 2261-2274
Pubmed: Author and Title
Google Scholar: Author Only Title Only Author and Title